

Simulation of strongly correlated systems with tensor network state methods

Mihály Máté, physicist MSc II



EÖTVÖS LORÁND UNIVERSITY
MSc THESIS

Supervisors:
Dr. Örs Legeza
Dr. Szilárd Szalay



MTA WIGNER RESEARCH CENTRE FOR PHYSICS

2017 May

Abstract

Due to the Nobel Prize in physics in 2016 the Haldane phase has become focused in the field of topological phases and strongly correlated systems. The simplest model showing the properties of this special phase is the widely studied bilinear-biquadratic model in a given range of the phase space. At a special point this model, known as AKLT model (after Affleck, Kennedy, Lieb and Tasaki), is integrable and its ground state gives the simplest structure among matrix product states (MPS). Analysing these kind of quantum systems the most powerful method is the density matrix renormalization group (DMRG) algorithm, which inherently represents the structure of MPS. Pair correlation and entanglement of spins are fundamental notions to study in strongly correlated systems, however, multipartite correlations can offer a much more essential and evident framework.

In my thesis the bilinear-biquadratic and the J_1 - J_2 Heisenberg model are investigated with the methods of multipartite correlations and entanglement using analytical techniques and DMRG algorithms. The exponents for multipartite correlation are determined in the different intervals of phase space (e.g. critical-, dimerised-, Haldane phase).

Contents

1	Introduction	2
1.1	Spin models	2
1.2	Numerical methods	4
1.3	Structure of the thesis	5
2	Multipartite correlations	5
2.1	Elementary subsystems	5
2.2	Bipartite systems	7
2.3	Bipartite measures	9
2.4	Structure of multipartite correlations	9
2.5	Multipartite measures	16
3	Density matrix renormalization group (DMRG)	18
4	Matrix product state (MPS)	20
4.1	Valence bond solid	22
5	Results	25
5.1	Spin-half J_1 - J_2 model	27
5.2	Bilinear-biquadratic model	34
6	Summary	45
	Acknowledgements	46
	References	47
	Certification in Hungarian	53

1 Introduction

The first intuitive model by which the transport phenomena in metals can be described was the naive but successful Drude model. Due to the development of quantum mechanics it became obvious that the classical idea, which considers the ions as fixed obstacles and the valence electrons as bouncing balls, could not be supported further. Sommerfeld was the one who described metals as ideal gases of electrons obeying Fermi–Dirac statistics. His model explains the specific heat and susceptibility of some common metals of simple structure. However, it turned out that the theory of magnetic systems and superconductivity needs to consider the interaction between electrons for the proper description. Moreover, beyond the time-honoured methods, e.g. mean field and perturbation theory, new mathematical and numerical frameworks have recently been developed for the treatment of *strongly correlated systems* [1]. Also, in quantum systems a special type of correlation occurs, which is called entanglement [2, 3].

The important goals of modern solid-state physics are to investigate the behaviour of spin and electron systems and to characterise the interactions in them; and also to improve models in order to fit the experimental results. By the tuning of the control parameters of the models novel phenomena can also be predicted, which have not been observed yet.

1.1 Spin models

The magnetic properties of solids can be described in the simplest way by the *Heisenberg model*. In this model atoms are represented as spins fixed on lattice sites. The internal structure of them is not taken into consideration, only the exchange interaction between them. The Hamilton operator is

$$H = J \sum_{\langle i,j \rangle} \mathbf{S}_i \mathbf{S}_j \quad (1)$$

if the coupling coefficient J is constant, and only the interaction between the nearest neighbours $\langle i,j \rangle$ contribute to the energy. The spin operator acting on the i -th site is $\mathbf{S}_i = (S_i^x, S_i^y, S_i^z)$, which obeys the commutation relation

$$[S_i^\alpha, S_j^\beta] = \delta_{ij} \sum_{\gamma} i \varepsilon^{\alpha\beta\gamma} S_j^\gamma \quad (2)$$

of the Lie algebra $\mathfrak{su}(2)$.

The sign of J determines whether the system is ferromagnetic ($J < 0$) or antiferromagnetic ($J > 0$). In the ferromagnetic ground state the spins are aligned, they point to the same direction. According to *Goldstone's theorem*, the breaking

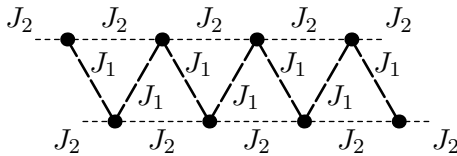


Figure 1: The illustration of couplings between lattice sites in the J_1 - J_2 Heisenberg model.

of the rotational symmetry results in a dispersion relation that starts from $k = 0$ without gap, e.g. for cubic lattice it is quadratic. In an antiferromagnetic material neighbouring spins tend to have opposite direction. In case of *Néel-type* order the spin structure is built up by two interlacing sublattices the net magnetization of which sum up to zero. The excitations start also at $k = 0$ without gap, however, the dispersion relation is linear.

Some well-known materials, e.g. graphite and quartz, exhibit huge anisotropy with respect to certain transport phenomena. Important novel results were the observation and construction of magnetic materials in which the exchange interaction is restricted to one direction. For instance, CsNiCl_3 behaves as an antiferromagnetic spin-one chain in which the spins are realized by the electron structure $3d^8$ of nickel ions Ni^{2+} [4, 5]. The quantum fluctuations can enlarge if the system is restricted to lower dimensions. In the one-dimensional isotropic Heisenberg model there is no ferromagnetic order except at zero temperature; in case of antiferromagnetic coupling the Néel order is unstable even though the temperature is zero, and the system exhibits the so-called spin liquid state.

The ground state of spin-half Heisenberg model in one dimension is exactly solvable by the Bethe ansatz, the excited states are obtained by spin flips. In the general Hamilton operator of $S > \frac{1}{2}$ isotropic systems, the besides the bilinear term, higher order terms have to be included that are invariant under $\text{SU}(2)$ symmetry. Models of these kinds are solvable analytically only for special choices of parameters. Consider a one-dimensional isotropic half-integer spin system which is invariant under translation by lattice constant. According to the *Lieb-Schultz-Mattis theorem* [6], the energy spectrum is gapless with non-degenerate ground state, or gapped and has degenerate ground state due to the breaking of the translational symmetry. Such degenerate ground state can be obtained if in the Heisenberg chain the *next nearest neighbour* interaction is also taken into account with a different coefficient J_2 . Then the Hamilton operator of this model is

$$H = J_1 \sum_i \mathbf{S}_i \mathbf{S}_{i+1} + J_2 \sum_i \mathbf{S}_i \mathbf{S}_{i+2}, \quad (3)$$

which is illustrated in figure 1. Frustration can occur in this system if the antiferromagnetic couplings are in the same order. One can give the exact solution of

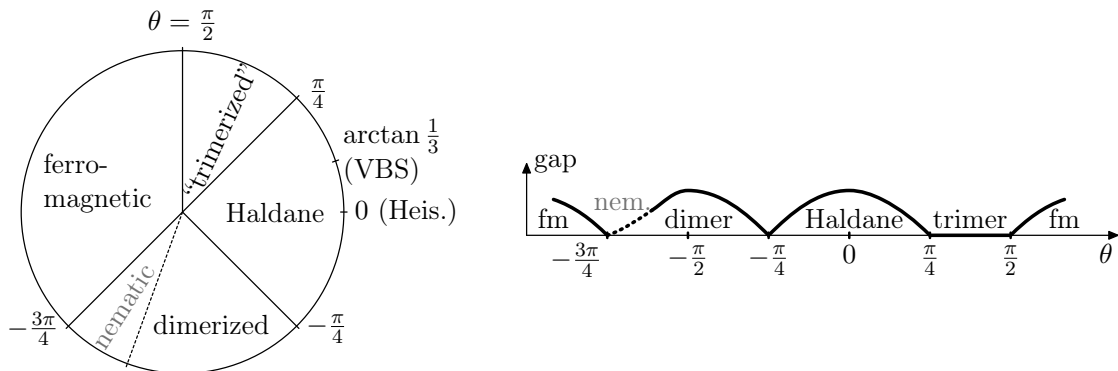


Figure 2: The schematic diagram of the phase space and the energy gap in term of θ for the bilinear-biquadratic model.

this model for spin-half chain at $J_2 = \frac{1}{2}J_1 > 0$, which is called *Majumdar–Ghosh model*. In this case the Hamilton operator (3) is the sum of projectors which maps onto the spin- $\frac{3}{2}$ subspace of three neighbouring spins [1], that is, the ground state is the tensor product of singlet states, which leads to the twofold degeneracy if open boundary conditions are assumed. An excited state can be obtained by breaking up a singlet bond, which process requires a given energy, therefore there is a gap in the dispersion relation. These excitations, called *spinons*, can move freely through the chain because the recombination of singlet bonds needs zero energy [7, 8].

The properties of half-integer spin systems can be explained through the spin-half Heisenberg model: the models are critical, excitations are just above the ground state. Haldane pointed out that the integer spin systems exhibit fundamentally different behaviour [9], which was one of his results honoured by the Nobel Prize in 2016. In the so-called *Haldane phase* there is a gap in the dispersion relation above the antiferromagnetic ground state, that is, the model is not critical and the correlation functions decay exponentially. This phase can be investigated by the widely studied *bilinear-biquadratic model*, which is the general model of spin-1 chains including nearest neighbour interaction:

$$H = \cos \theta \sum_i \mathbf{S}_i \mathbf{S}_{i+1} + \sin \theta \sum_i (\mathbf{S}_i \mathbf{S}_{i+1})^2. \quad (4)$$

The interaction can be tuned by the parameter θ , leading to a diverse phase diagram, seen in figure 2. The different phases are discussed in section 5.2.

1.2 Numerical methods

The aforementioned models, as usual in physics, are solvable exactly only in restricted regions of the phase space of the parameters. Analytical approxima-

tions can be obtained, however, for example, perturbation theory cannot provide a general treatment for strongly correlated systems.

In the recent decades many numerical methods have been improved which are specified on low-dimensional systems. The straightforward method is the *exact diagonalization* of the Hamilton operator, in which the cost of the calculation scales exponentially with the number of sites. Despite applying optimized iterative algorithms, only an order of ten sites can be handled, which is insufficient for the description of the system. Therefore finite-size scaling has to be used to extrapolate to the thermodynamic limit. Accordingly, we need a method which finds the appropriate representation of a system on a restricted Hilbert space. Wilson developed the *numerical renormalization group* (NRG) method by which impurity problems were able to be handled. He was awarded the Nobel Prize in 1975 for his results in the solution of the Kondo problem. However, due to the bad scaling of numerical errors the application of the NRG algorithm is limited. The major breakthrough was the development of *density matrix renormalization group* (DMRG) method by White in the 90s [10, 11]. Nowadays the most efficient method for the treatment of low-dimensional strongly correlated systems is the DMRG algorithm, by which chains of hundreds of sites can be modelled. This algorithm inherently provides the *matrix product state* (MPS) representation of the wave function, which is discussed in the further sections. The dimensions of matrices depend on the strength of the entanglement in the system.

1.3 Structure of the thesis

In this thesis, first, I recall the theoretical background of multipartite correlation and entanglement, which will serve as a method for the investigation of spin chains. Then, I discuss the DMRG and MPS based methods I implemented and used during my research presented here. After this I apply the theory of multipartite correlation for the investigation of spin chains for the first time in the literature. I calculate the decay of the different two-, three- and four-site correlations for several parameter values of the models (3) and (4) by the use of the implementations developed by myself. Finally, I summarize the further plans and opportunities.

2 Multipartite correlations

2.1 Elementary subsystems

Quantum mechanics gives a statistical description of a system. The expectation value of physical quantities can be calculated by the *state vector* which represents

our knowledge of the system [12, 13, 14].

A system is *pure* if there is a non-degenerate Neumann measurement that gives the same result when it is repeated on the different copies of that system. Systems having this property are represented by a *pure state* $\pi = |\psi\rangle\langle\psi|$, where $|\psi\rangle$ is a normalised element of Hilbert space \mathcal{H} ($\langle\psi|\psi\rangle = 1$), which is supposed to be final in this thesis. The set of pure states is

$$\mathcal{P}(\mathcal{H}) := \left\{ \pi \in \text{Lin}_{\text{SA}} \mathcal{H} \mid \pi^2 = \pi, \text{Tr} \pi = 1 \right\}. \quad (5)$$

The expectation value of a physical quantity, represented by operator O , can be evaluated on a pure system as $\langle\psi|O|\psi\rangle = \text{Tr}(\pi O)$.

If a system can not be described by a pure state, than it is represented by *mixed state*, which is the convex combination (statistical mixture) of pure states. In general, the *state* of a system is in the set

$$\mathcal{D}(\mathcal{H}) := \text{Conv} \mathcal{P}(\mathcal{H}) \equiv \left\{ \varrho = \varrho^\dagger \mid \pi_i \in \mathcal{P}(\mathcal{H}), p_i \geq 0, \|\mathbf{p}\|_1 = 1 : \varrho = \sum_i p_i \pi_i \right\}. \quad (6)$$

Consequently, the mixed states are such positive semidefinite linear operators that are also self-adjoint and normalised ($\text{Tr} \varrho = 1$); the expectation value of O is

$$\langle O \rangle = \text{Tr}(\varrho O) = \sum_i p_i \text{Tr}(\pi_i O) = \sum_i p_i \langle\psi_i|O|\psi_i\rangle. \quad (7)$$

To quantify the mixedness of a state $\varrho \in \mathcal{D}$, entropic quantities are introduced. In classical information theory the well-known *Shannon entropy* measures the information content of a system. The corresponding quantity in quantum mechanics is the so-called *von Neumann entropy*,

$$S(\varrho) := -\text{Tr}(\varrho \ln \varrho), \quad (8)$$

having beneficent properties: non-negative, continuous, additive for uncorrelated states, faithful (zero iff the state is pure), non-decreasing in bistochastic quantum channels [15, 16].

The (measure of) *distinguishability* of two states ($\varrho, \sigma \in \mathcal{D}$) is the *Umegaki relative entropy*,

$$D(\varrho|\sigma) = \text{Tr}[\varrho(\ln \varrho - \ln \sigma)], \quad (9)$$

which is also non-negative, zero iff $\varrho = \sigma$, non-decreasing in bistochastic quantum channels [17, 18].

2.2 Bipartite systems

One of the most characteristic manifestations of the non-classical nature of quantum systems is the non-classical behaviour of the correlations among the subsystems. Let us introduce the corresponding notions in the simplest, *bipartite* case first. The state vector representing the composition of two elementary subsystems is the normalized element of the tensor product Hilbert space $\mathcal{H}_{12} = \mathcal{H}_1 \otimes \mathcal{H}_2$. Similarly, the set of pure states $\mathcal{P}_1 := \mathcal{P}(\mathcal{H}_1)$, $\mathcal{P}_2 := \mathcal{P}(\mathcal{H}_2)$, $\mathcal{P}_{12} := \mathcal{P}(\mathcal{H}_{12})$ and the set of mixed states \mathcal{D}_1 , \mathcal{D}_2 , \mathcal{D}_{12} are understood. The reduced state of state $\varrho \in \mathcal{D}_{12}$ can be obtained by the partial trace operation: $\varrho_1 = \text{Tr}_2 \varrho$, where $\text{Tr}_2 : \mathcal{D}_{12} \rightarrow \mathcal{D}_1$ is linear and for elementary tensor $A \otimes B$ the operation is $\text{Tr}_2(A \otimes B) = A \text{Tr} B$ [12, 14].

The *correlation* of two random variable is $\langle O_1 O_2 \rangle - \langle O_1 \rangle \langle O_2 \rangle$. (In mathematical terminology this is called covariance, and the normalized covariance is the correlation.) In quantum mechanics the correlation of two observables measured on different subsystems is

$$C(\varrho; O_1, O_2) := \langle O_1 \otimes O_2 \rangle - \langle O_1 \rangle \langle O_2 \rangle = \text{Tr} [(\varrho - \varrho_1 \otimes \varrho_2) O_1 \otimes O_2]. \quad (10)$$

A bipartite system is uncorrelated if this expression vanishes for all pairs of observables, leading to $\varrho = \varrho_1 \otimes \varrho_2$. Therefore the set of *uncorrelated states* is

$$\mathcal{D}_{\text{unc}} := \left\{ \varrho \in \mathcal{D}_{12} \mid \exists \varrho_1 \in \mathcal{D}_1, \exists \varrho_2 \in \mathcal{D}_2 : \varrho = \varrho_1 \otimes \varrho_2 \right\}. \quad (11)$$

All classical pure states are uncorrelated. In quantum systems, however, $\mathcal{P}_{\text{unc}} := \mathcal{D}_{\text{unc}} \cap \mathcal{P}_{12} \neq \mathcal{P}_{12}$, that is, pure states can be correlated, which is called *entanglement* (for pure state). The uncorrelated pure states are also named *separable pure states*,

$$\mathcal{P}_{\text{sep}} \equiv \mathcal{P}_{\text{unc}} = \left\{ \pi \in \mathcal{P}_{12} \mid \exists \pi_1 \in \mathcal{P}_1, \exists \pi_2 \in \mathcal{P}_2 : \pi = \pi_1 \otimes \pi_2 \right\}; \quad (12)$$

the others are *entangled*, $\overline{\mathcal{P}_{\text{sep}}} = \mathcal{P}_{12} \setminus \mathcal{P}_{\text{sep}}$.

In general (not only for pure states) the *separable states* are the mixture of separable pure ones, or equivalently, the the mixture of uncorrelated states [19]:

$$\mathcal{D}_{\text{sep}} := \text{Conv} \mathcal{P}_{\text{sep}} = \text{Conv} \mathcal{D}_{\text{unc}}. \quad (13)$$

The definition is motivated by the transformation called “*local operation and classical communication*” (*LOCC*), which can create such kind of states. The classical communication corresponds to classical interaction, while quantum correlation is generated by quantum interaction, that is, separable states do not have quantum correlations from this point of view. A state is entangled if it is not separable, so the set of *entangled states* are $\overline{\mathcal{D}_{\text{sep}}} = \mathcal{D}_{12} \setminus \mathcal{D}_{\text{sep}}$.

To sum up, the structure of bipartite state spaces are the following.

$$\begin{aligned} \mathcal{P}_{12} &\subseteq \mathcal{D}_{12} \equiv \text{Conv } \mathcal{P}_{12} \\ \mathcal{P}_{\text{unc}} \equiv \mathcal{P}_{\text{sep}} &\subseteq \mathcal{D}_{\text{unc}} \subseteq \mathcal{D}_{\text{sep}} \equiv \text{Conv } \mathcal{P}_{\text{sep}} \end{aligned} \quad (14)$$

An arbitrary state vector can be expanded on the orthonormal bases $\{|\varphi_{1,\gamma_1}\rangle\}$ and $\{|\varphi_{2,\gamma_2}\rangle\}$:

$$|\psi\rangle = \sum_{\gamma_1=1}^{d_1} \sum_{\gamma_2=1}^{d_2} \psi_{\gamma_1\gamma_2} |\varphi_{1,\gamma_1}\rangle \otimes |\varphi_{2,\gamma_2}\rangle. \quad (15)$$

One can apply the singular value decomposition on the coefficient matrix, that is $\psi = \mathbf{U}\mathbf{S}\mathbf{V}^\dagger$, where $\mathbf{U} \in U(d_1)$ and $\mathbf{V} \in U(d_2)$ are unitary matrices, \mathbf{S} is diagonal having non-negative s_α entries called the singular values of ψ . By this the state vector can be expressed as

$$|\psi\rangle = \sum_{\alpha=1}^{\min(d_1,d_2)} s_\alpha |\varphi'_{1,\alpha}\rangle \otimes |\varphi'_{2,\alpha}\rangle, \quad (16)$$

which is commonly known as *Schmidt decomposition*. The eigenvalues of the reduced state are s_α^2 , the eigenstates are $\{|\varphi'_{1,\alpha}\rangle\}$ and $\{|\varphi'_{2,\alpha}\rangle\}$. So that it is easy to decide whether a pure state is separable or not:

$$\pi \in \mathcal{P}_{\text{sep}} \iff \text{Tr}_2 \pi \in \mathcal{P}_1 \iff \text{Tr}_1 \pi \in \mathcal{P}_2. \quad (17)$$

For example, let $|\psi_1\rangle, |\psi'_1\rangle \in \mathcal{H}_1$ and $|\psi_2\rangle, |\psi'_2\rangle \in \mathcal{H}_2$ be two orthonormal pairs of state vectors.

- i) The state vector $|\psi\rangle = |\psi_1\rangle \otimes |\psi_2\rangle \in \mathcal{H}_{12}$ is an elementary tensor, so the state $\pi = |\psi\rangle\langle\psi|$ is separable, that is,

$$\begin{aligned} \text{Tr}_2 \pi &= |\psi_1\rangle\langle\psi_1| \in \mathcal{P}_1 \\ \text{Tr}_1 \pi &= |\psi_2\rangle\langle\psi_2| \in \mathcal{P}_2 \end{aligned} \quad \pi = \pi_1 \otimes \pi_2 \in \mathcal{P}_{\text{sep}}. \quad (18a)$$

- ii) On the other hand, if $|\psi\rangle = \frac{1}{\sqrt{2}}(|\psi_1\rangle \otimes |\psi_2\rangle + |\psi'_1\rangle \otimes |\psi'_2\rangle) \in \mathcal{H}_{12}$, the pure state $\pi = |\psi\rangle\langle\psi|$ is entangled because

$$\begin{aligned} \text{Tr}_2 \pi &= \frac{1}{2}(|\psi_1\rangle\langle\psi_1| + |\psi'_1\rangle\langle\psi'_1|) \notin \mathcal{P}_1 \\ \text{Tr}_1 \pi &= \frac{1}{2}(|\psi_2\rangle\langle\psi_2| + |\psi'_2\rangle\langle\psi'_2|) \notin \mathcal{P}_2 \end{aligned} \quad \pi \neq (\text{Tr}_2 \pi) \otimes (\text{Tr}_1 \pi) \quad (18b)$$

2.3 Bipartite measures

After introducing the notions of uncorrelated (11) and separable states (13), our aim is to quantify the correlation and the entanglement of the states.

The correlation of two physical quantity was defined previously (10), however, we want to give how the state ϱ itself is correlated. Let the correlation of the state be the distinguishability from the uncorrelated ones using the relative entropy (9):

$$\min_{\sigma \in \mathcal{D}_{\text{unc}}} D(\varrho || \sigma) = S(\varrho_1) + S(\varrho_2) - S(\varrho) = I(\varrho). \quad (19)$$

The minimum of the relative entropy is attained when $\sigma = \varrho_1 \otimes \varrho_2$ [20], leading to that the correlation of the state can be expressed as the sum of the entropies. This quantity is known as the (*quantum*) *mutual information* [14].

Since the entanglement of a pure state is the correlation, then let the measure of the entanglement be the measure of the correlation of the state,

$$E|_{\mathcal{P}}(\pi) := I|_{\mathcal{P}}(\pi) = 2S(\pi_1) = 2S(\pi_2), \quad (20)$$

which is the double of the *entanglement entropy* [21]. Due to the Schmidt decomposition (16) the (non-zero part of the) spectra of the marginals of pure states are equal. For mixed states the average entanglement of the optimal pure decomposition is a natural definition for the role of the entanglement measure [22].

$$E(\varrho) = \min \left\{ \sum_i p_i I|_{\mathcal{P}}(\pi_i) \mid \pi_i \in \mathcal{P}_{12}, p_i \geq 0, \|\mathbf{p}\|_1 = 1 : \sum_i p_i \pi_i = \varrho \right\} \quad (21)$$

The minimization, which is a hard numerical problem, takes place over the entire set of the possible decompositions, and this approach is called convex roof extension. This measure is appropriate because it is non-increasing for LOCC transformations so it expresses the quantum nature of the entanglement, being a correlation cannot be increased by classical interaction.

The measures are *faithful*, that is, I and E are zero iff the state is uncorrelated and separable, respectively. The inequality $E \leq I$ reveals that some part of the correlation of a system is the quantum entanglement.

2.4 Structure of multipartite correlations

In the following sections we discuss the extension of the bipartite notions to multipartite case, resulting in a four-level lattice structure [23, 24].

A *partially ordered set*, or *poset*, is a set P endowed with a *partial order* \preceq (reflexive, antisymmetric, transitive) relation. If *greatest lower bound* (infimum) and *least upper bound* (supremum) exist uniquely for all pairs of elements in the poset, then the structure is called a *lattice* [25, 26]. For example, in the set of integers the divisibility is a possible partial order, the infimum is the greatest common divisor, the supremum is the lowest common multiple.

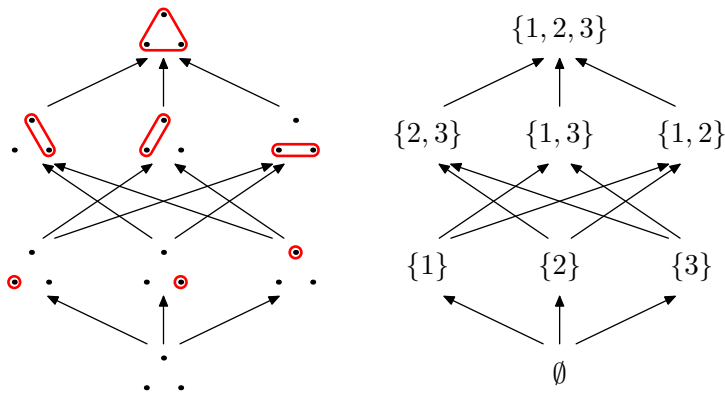


Figure 3: The lattice of power set $P_0(\{1, 2, 3\})$.

2.4.1 Level 0: subsystems

For n -partite system let the labels of the *elementary subsystems* be denoted by $i \in L = \{1, 2, \dots, n\}$ and the associated Hilbert spaces are \mathcal{H}_i . A *subsystem* (not elementary in general) is labelled by $X \subseteq L$, so we have the Hilbert space $\mathcal{H}_X = \bigotimes_{i \in X} \mathcal{H}_i$ and states $\mathcal{D}_X := \mathcal{D}(\mathcal{H}_X)$. Every label X is an element of the power set of L , given as

$$P_0(L) := 2^L, \quad (22)$$

which is a basic example for a lattice structure with respect to set inclusion, intersection and union.

Let us write out the tripartite case. The size of the power set of $L = \{1, 2, 3\}$ is eight. Its lattice structure is shown in Figure 3, where the encircled black dots illustrate the elements of the power set, the arrow symbolizes the partial order (inclusion).

2.4.2 Level I: partitions

The only possible way of partitioning of a bipartite system, and the corresponding notions of correlation and entanglement, were shown in section 2.2. Now, our aim is to extend these notions for all the different partitionings of an arbitrary, n -partite system.

A *partition* of the system is a set $\xi = \{X_1, X_2, \dots, X_{|\xi|}\}$ (with the shorthand notation $\xi = X_1 | X_2 | \dots | X_{|\xi|}$) having *parts* $X \subseteq L$ that are non-empty (i), disjoint (ii) and together amount to the whole system L (iii). The set of all possible

partitions of the system is

$$P_1(L) := \left\{ \xi = X_1 | X_2 | \dots | X_{|\xi|} \mid \begin{array}{l} \forall X \in P_0 \setminus \{\emptyset\}, \quad (\text{i}) \\ \forall X \neq X' \in \xi : X \cap X' = \emptyset, \quad (\text{ii}) \\ \bigcup_{X \in \xi} X = L \quad (\text{iii}) \end{array} \right\}. \quad (23)$$

For two partitions $\xi, \nu \in P_1$, one can say ν is the *refinement* of ξ (or “ ν is finer than ξ ” or “ ξ is coarser than ν ”), if ξ can be obtained by joining some parts of ν . That is, the partial order

$$\nu \preceq \xi \stackrel{\text{def}}{\iff} \forall Y \in \nu \quad \exists X \in \xi : Y \subseteq X \quad (24)$$

is introduced. It can be shown that the set of partitions is a lattice w.r.t. the refinement.

In accordance with the definition (11), the set of ξ -uncorrelated states is

$$\mathcal{D}_{\xi\text{-unc}} := \left\{ \varrho \in \mathcal{D} \mid \forall X \in \xi, \exists \varrho_X \in \mathcal{D}_X : \varrho = \bigotimes_{X \in \xi} \varrho_X \right\}, \quad (25)$$

resulting arbitrary O_X observables of corresponding subsystems X are uncorrelated: $\langle \bigotimes_{X \in \xi} O_X \rangle = \prod_{X \in \xi} \langle O_X \rangle$.

As the generalization of (10), introduce the correlation of observables O_i ($i \in L$) defined in elementary subsystems with respect to ξ partition:

$$C_\xi(\varrho; O_1, \dots, O_n) = \left\langle \bigotimes_{i \in L} O_i \right\rangle - \prod_{X \in \xi} \left\langle \bigotimes_{i \in X} O_i \right\rangle = \text{Tr} \left[\left(\varrho - \bigotimes_{X \in \xi} \varrho_X \right) \bigotimes_{i \in L} O_i \right]. \quad (26)$$

Following definition (13), the ξ -separable states are the mixtures of ξ -uncorrelated ones [27, 28, 29, 30, 31, 32],

$$\mathcal{D}_{\xi\text{-sep}} := \text{Conv } \mathcal{D}_{\xi\text{-unc}}, \quad (27)$$

exhibiting the lack of quantum correlation among the parts $X \in \xi$. Corollary, the set $\mathcal{D}_{\xi\text{-sep}}$ is closed under LOCC transformation.

If a state is uncorrelated w.r.t. a partition, then it is uncorrelated w.r.t. every coarser partition, that is,

$$\nu \preceq \xi \iff \mathcal{D}_{\nu\text{-unc}} \subseteq \mathcal{D}_{\xi\text{-unc}}. \quad (28a)$$

Because of (27), the similar expression follows for ξ -separable states [23, 24]:

$$\nu \preceq \xi \iff \mathcal{D}_{\nu\text{-sep}} \subseteq \mathcal{D}_{\xi\text{-sep}}. \quad (28b)$$

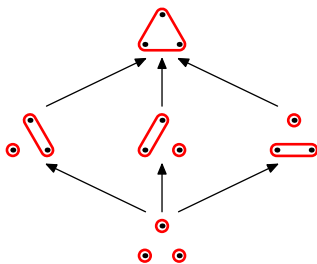


Figure 4: The lattice structure of the partitions of a tripartite system $P_1(\{1, 2, 3\})$.

Consequently, the sets of state-sets, $\mathcal{D}_{\xi\text{-unc}}$ and $\mathcal{D}_{\xi\text{-sep}}$ corresponding to different partitions ξ , form lattices that are isomorphic to the lattice of partitions $P_1(L)$.

Let us write out the tripartite case. The number of elements of P_1 set can be given by the Bell numbers having the recursion $B_{n+1} = \sum_{k=0}^n \binom{n}{k} B_k$ ($B_0 = B_1 = 1$). There are five possible combinations of parts $X \in P_0(\{1, 2, 3\})$ to form the full system:

$$P_1(\{1, 2, 3\}) = \left\{ 1|2|3, 12|3, 13|2, 23|1, 123 \right\}. \quad (29)$$

Endowing this set with the refinement we have: $1|2|3 \preceq ab|c \preceq 123$ ($a, b, c \in \{1, 2, 3\}$). These partitions are shown in figure 4.

2.4.3 Level II: sets of partitions

Consider the previous $n = 3$ example. Let us have a state $\rho \notin \mathcal{D}_{ab|c\text{-sep}}$, meaning it is neither the convex combination of $12|3$ - nor of $13|2$ - nor of $23|1$ -uncorrelated states. However, a crucial observation in the theory of multipartite entanglement is that there are such $\rho \notin \mathcal{D}_{ab|c\text{-sep}}$ states that can be mixed with the *simultaneous* use of $12|3$ -, $13|2$ -, $13|2$ -uncorrelated states, that is, $\rho \in \text{Conv}(\mathcal{D}_{12|3\text{-unc}} \cup \mathcal{D}_{13|2\text{-unc}} \cup \mathcal{D}_{23|1\text{-unc}})$. Such states should not be considered as fully tripartite-entangled ones [29, 30, 31, 32, 23], since there is no need for tripartite-entangled states to mix them, so further notions of correlation have to be introduced; this leads to the Level II structure.

Let $\xi = \{\xi_1, \xi_2, \dots, \xi_{|\xi|}\}$ be a non-empty subset of P_1 that includes every partitions that are finer then its maximal element(s). The collection of these subsets (called *down-sets* or *ideals*) is

$$P_{\text{II}}(L) := \mathcal{O}_{\downarrow}(P_1(L)) \setminus \{\emptyset\} \equiv \left\{ \xi \in 2^{P_1(L)} \setminus \{\emptyset\} \mid \forall \xi \in \xi : v \preceq \xi \Rightarrow v \in \xi \right\}. \quad (30)$$

In the figure of P_1 a down-set is closed under following the arrows backwards.

A partial order \preceq in the set P_{II} is the set-inclusion (\subseteq), that is, $\xi \preceq \nu \Leftrightarrow \xi \subseteq \nu$. Together with the intersection (\cap) and union (\cup) one can prove that P_{II} is a lattice.

A state ϱ is ξ -uncorrelated if it is uncorrelated for at least one $\xi \in \xi$ partition ($\varrho \in \mathcal{D}_{\xi\text{-unc}}$), so we have

$$\mathcal{D}_{\xi\text{-unc}} := \bigcup_{\xi \in \xi} \mathcal{D}_{\xi\text{-unc}} \stackrel{(28a)}{=} \bigcup_{\xi \in \max \xi} \mathcal{D}_{\xi\text{-unc}}. \quad (31)$$

We introduce the correlation of observables O_i ($i \in L$) defined in elementary subsystems with respect to ξ down-set:

$$C_{\xi}(\varrho; O_1, \dots, O_n) = \min_{\xi \in \xi} C_{\xi}(\varrho; O_1, \dots, O_n). \quad (32)$$

Following definition (27) a state is ξ -separable if it is the mixture of ξ -uncorrelated states, so it is the element of

$$\mathcal{D}_{\xi\text{-sep}} := \text{Conv } \mathcal{D}_{\xi\text{-unc}}, \quad (33)$$

which is closed under LOCC transformation as is was observed for ξ -separable in (27) [23].

Similarly to (28a) and (28b), the following isomorphisms can be derived [23, 24]:

$$\nu \preceq \xi \iff \mathcal{D}_{\nu\text{-unc}} \subseteq \mathcal{D}_{\xi\text{-unc}}, \quad (34a)$$

$$\nu \preceq \xi \iff \mathcal{D}_{\nu\text{-sep}} \subseteq \mathcal{D}_{\xi\text{-sep}}. \quad (34b)$$

The number of possible down-sets rapidly increases with the number of subsystems but there are some down-sets, and corresponding state sets, that have expressive meaning. A partition is k -partitionable if the number of its parts is at least k . The set of these partitions is

$$\mu_k := \{\mu \in P_{\text{I}} \mid |\mu| \geq k\} \in P_{\text{II}}, \quad (35)$$

and the corresponding states are the k -partitionably uncorrelated states $\mathcal{D}_{k\text{-part, unc}} := \mathcal{D}_{\mu_k\text{-unc}}$ and the k -partitionably separable states $\mathcal{D}_{k\text{-part, sep}} := \mathcal{D}_{\mu_k\text{-sep}}$.

The k' -producibility, which is a dual property in a certain sense, sets a maximum size to every parts, that is

$$\nu_{k'} := \{\nu \in P_{\text{I}} \mid \forall N \in \nu : |N| \leq k'\} \in P_{\text{II}}, \quad (36)$$

and the corresponding states are k' -producibly uncorrelated ones $\mathcal{D}_{k'\text{-prod, unc}} := \mathcal{D}_{\nu_{k'}\text{-unc}}$ and k' -producibly separable ones $\mathcal{D}_{k'\text{-prod, sep}} := \mathcal{D}_{\nu_{k'}\text{-sep}}$.

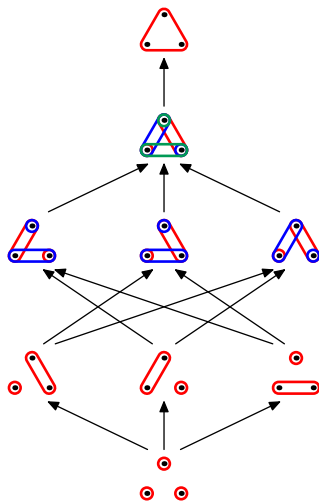


Figure 5: The lattice diagram corresponding to the P_{II} set.

Let us write out the tripartite case. Since the maximal elements of a non-empty down-set ($\max \xi$) uniquely determines the down-set itself, the $\xi = \downarrow \max \xi$ shorthand notation can be used:

$$\begin{aligned}
 P_{\text{II}} = \{ & \downarrow\{123\} = P_1, \\
 & \downarrow\{12|3, 13|2, 23|1\}, \\
 & \downarrow\{12|3, 13|2\}, \downarrow\{12|3, 23|1\}, \downarrow\{13|2, 23|1\}, \\
 & \downarrow\{12|3\}, \downarrow\{23|1\}, \downarrow\{23|1\}, \\
 & \downarrow\{1|2|3\} = \{1|2|3\} \\
 & \}.
 \end{aligned} \tag{37}$$

The illustration in figure 5 shows the maximal elements of the P_{II} labels.

The relation of partitionability and producibility is demonstrated with the lining of the P_1 lattice in figure 6. The two notions coincide for bi- and tripartite cases.

2.4.4 Level III: entanglement classes

For the completeness of this section the Level III type lattice structure ought to be mentioned, although being not studied in this thesis. The introduced notions of entanglement result in containing sets (34b), that is, the *sufficient* set of ξ -uncorrelated states is given by which the a state can be mixed. Moreover, all the possible intersections of ξ -separable states can be constructed (*entanglement classes*) that determine the *necessary and sufficient* set of ξ -uncorrelated states for the mixing.

One can derive that the labelling of the entanglement classes are the up-sets (or *filters*) of P_{II} [23]. This generates the coarsening of the LOCC classification: if

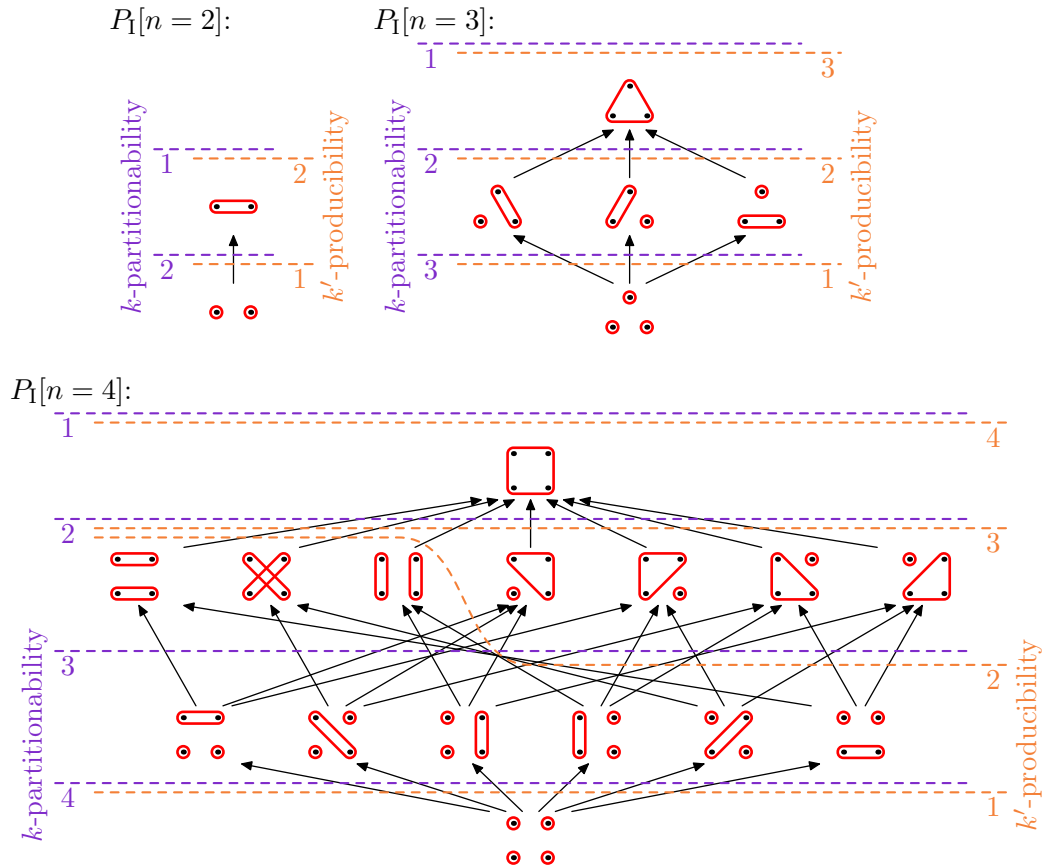


Figure 6: The illustration of partitionability and producibility on the diagram of P_1 lattice. The k -partitionable partitions are below the k -th lilac line, the k' -producible ones are below the k' -th orange line. For $n > 3$ the two notions are different.

there is an LOCC transformation bringing a state from a class to an other, than these classes are in relation w.r.t. to that of this lattice [23].

2.5 Multipartite measures

2.5.1 Level 0: subsystems

With the aid of the relative entropy, defined in (9), correlation and entanglement measures can be formulated in the same way as in the bipartite case. This leads to measures given in the terms of entropies (8) of states of subsystems $X \in P_0$. This is summarized in the forthcoming sections.

2.5.2 Level I: partitions

The introduction of correlation and entanglement of a system w.r.t. a partition $\xi = X_1|X_2|\dots|X_{|\xi|}$ follows easily from the basic ideas discussed in section 2.3. The correlation of a state $\varrho \in \mathcal{D}$ w.r.t. a partition ξ , or ξ -correlation (ξ -mutual information) for short, is the measure of distinguishability from the ξ -uncorrelated states [20, 23]:

$$I_\xi(\varrho) := \min_{\sigma \in \mathcal{D}_{\xi\text{-unc}}} D(\varrho||\sigma) = \sum_{X \in \xi} S(\varrho_X) - S(\varrho). \quad (38)$$

(The second equality is that the minimal value is attained when $\sigma = \bigotimes_{X \in \xi} \varrho_X$ [20].)

The ξ -entanglement is defined as the convex roof extension of the pure state restriction of the ξ -correlation [23],

$$E_\xi(\varrho) = \min \left\{ \sum_i p_i I_\xi|_{\mathcal{P}}(\pi_i) \mid \pi_i \in \mathcal{P}_L, p_i \geq 0, \|\mathbf{p}\|_1 = 1 : \sum_i p_i \pi_i = \varrho \right\}, \quad (39)$$

which is also non-increasing w.r.t. LOCC transformations. These quantities are faithful, that is, I_ξ and E_ξ are zero iff the state is ξ -uncorrelated and ξ -separable, respectively. Furthermore, $E_\xi \leq I_\xi$ holds.

One can prove the *multipartite monotonicity* of ξ -correlation and ξ -entanglement [23, 24],

$$v \preceq \xi \iff I_v \geq I_\xi, \quad (40a)$$

$$v \preceq \xi \iff E_v \geq E_\xi, \quad (40b)$$

that is, for finer partitions the states are more correlated and entangled. Hence, the set of functions describing correlation and entanglement has the same structure as that of P_1 lattice.

2.5.3 Level II: sets of partitions

To give the amount of correlation and entanglement w.r.t. up-sets $\xi = \{\xi_1, \xi_2, \dots, \xi_{|\xi|}\}$, we extend the quantities introduced in section 2.5.2. So, the ξ -correlation (ξ -mutual information) of a state $\varrho \in \mathcal{D}$ is the measure of distinguishability from the ξ -uncorrelated states [23, 24]:

$$I_\xi(\varrho) = \min_{\sigma \in \mathcal{D}_{\xi\text{-unc}}} D(\varrho||\sigma) = \min_{\xi \in \xi} \min_{\sigma \in \mathcal{D}_{\xi\text{-unc}}} D(\varrho||\sigma) = \min_{\xi \in \xi} \sum_{X \in \xi} S(\varrho_X) - S(\varrho). \quad (41)$$

The second equality means that the minimization over the union of sets (31) is equivalent to minimizing over each set and having the lowest value.

The ξ -entanglement is the convex roof extension of the pure state restriction of the ξ -correlation [23]:

$$E_\xi(\varrho) = \min \left\{ \sum_i p_i I_\xi |_{\mathcal{P}}(\pi_i) \mid \pi_i \in \mathcal{P}_L, p_i \geq 0, \|\mathbf{p}\|_1 = 1 : \sum_i p_i \pi_i = \varrho \right\}, \quad (42)$$

that is also non-increasing w.r.t. LOCC transformations.

These quantities are faithful again, that is, I_ξ and E_ξ is zero if and only if the state is ξ -uncorrelated and ξ -separable, respectively. The inequality $E_\xi \leq I_\xi$ also holds.

One can prove the *multipartite monotonicity* of ξ -correlation and ξ -entanglement [23, 24],

$$\mathbf{v} \preceq \xi \iff I_{\mathbf{v}} \geq I_\xi, \quad (43a)$$

$$\mathbf{v} \preceq \xi \iff E_{\mathbf{v}} \geq E_\xi. \quad (43b)$$

For the particular elements $\mu_k, \nu_{k'}$ of set P_{II} the measures are derived following definitions (35) and (36). The k -partitionability correlation and the k' -producibility correlation are [24]

$$I_{k\text{-part}}(\varrho) := I_{\mu_k}(\varrho) = \min_{|\mu| \geq k} I_\mu(\varrho), \quad (44a)$$

$$I_{k\text{-prod}}(\varrho) := I_{\nu_{k'}}(\varrho) = \min_{\forall N \in \nu: |N| \leq k'} I_\nu(\varrho); \quad (44b)$$

and the k -partitionability entanglement and the k' -producibility entanglement are

$$E_{k\text{-part}}(\varrho) := E_{\mu_k}(\varrho), \quad (45a)$$

$$E_{k'\text{-prod}}(\varrho) := E_{\nu_{k'}}(\varrho). \quad (45b)$$

The multipartite monotonicity can be expressed as inequalities of k, k' parameters:

$$\mu_k \preceq \mu_l \iff k \geq l \iff I_{k\text{-part}} \geq I_{l\text{-part}}, \quad (46a)$$

$$\nu_{k'} \preceq \nu_{l'} \iff k' \leq l' \iff I_{k'\text{-prod}} \geq I_{l'\text{-prod}}, \quad (46b)$$

$$\mu_k \preceq \mu_l \iff k \geq l \iff E_{k\text{-part}} \geq E_{l\text{-part}}, \quad (46c)$$

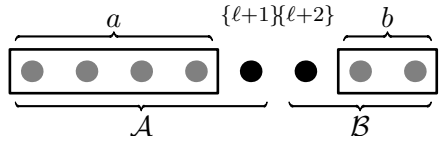
$$\nu_{k'} \preceq \nu_{l'} \iff k' \leq l' \iff E_{k'\text{-prod}} \geq E_{l'\text{-prod}}. \quad (46d)$$

3 Density matrix renormalization group (DMRG)

The previously introduced new framework has already been applied to study the electronic structure of molecules [24]. In this thesis it is being used for the examination of spin chains, which are numerically handled by the powerful DMRG method.

The solution of the Kondo problem brought the Nobel Prize for Wilson, although the desired universality of NRG did not come to fruition. In 1992 the NRG method was rethought by White and the fundamentals of DMRG algorithm was laid down. One of the basic ideas was to add environment to the spin chain being renormalized, and the other one was to select the basis states via truncation by the use of Schmidt decomposition [10, 11].

The state vector representing a chain of length N is expanded on the basis



$$|\psi_{a,\gamma_a}\rangle \otimes |\psi_{\{\ell+1\},\gamma_{\{\ell+1\}}}\rangle \otimes |\psi_{\{\ell+2\},\gamma_{\{\ell+2\}}}\rangle \otimes |\psi_{b,\gamma_b}\rangle, \quad (47)$$

where $a = \{1, \dots, \ell\}$ denotes the *left block* consisting of ℓ lattice point, $\psi_{\{\ell+1\}}$ and $\psi_{\{\ell+2\}}$ are two one-point states, $b = \{\ell + 3, \dots, N\}$ is the *right block*. This scheme is the so-called *superblock* representation, symbolized by $a\bullet\bullet b$, which is also illustrated in figure 7. By the diagonalization of the full-chain Hamilton operator one can obtain the eigenstate to be examined, which is usually the ground state. This is called the *target state* of the DMRG and represented in the basis (47) as

$$\begin{aligned} |\psi\rangle &= \sum_{\gamma_a, \gamma_{\{\ell+1\}}, \gamma_{\{\ell+2\}}, \gamma_b} c_{\gamma_a, \gamma_{\{\ell+1\}}, \gamma_{\{\ell+2\}}, \gamma_b} |\psi_{a,\gamma_a}\rangle \otimes |\psi_{\{\ell+1\},\gamma_{\{\ell+1\}}}\rangle \otimes |\psi_{\{\ell+2\},\gamma_{\{\ell+2\}}}\rangle \otimes |\psi_{b,\gamma_b}\rangle \\ &\equiv \sum_{\gamma_A, \gamma_B} c_{\gamma_A, \gamma_B} |\varphi_{A,\gamma_A}\rangle \otimes |\varphi_{B,\gamma_B}\rangle, \end{aligned} \quad (48)$$

where the states of subsystems $a\bullet$ and $\bullet b$ are $|\varphi_{A,\gamma_A}\rangle$ and $|\varphi_{B,\gamma_B}\rangle$, respectively. Within one renormalization step the partial trace operation is applied to get the reduced density matrix of subsystem \mathcal{A} , which is

$$\rho_{\mathcal{A}} = \text{Tr}_{\mathcal{B}} |\psi\rangle\langle\psi| = \sum_{\gamma_A, \gamma'_A} \left(\sum_{\gamma_B} c_{\gamma_A, \gamma_B} c_{\gamma'_A, \gamma_B}^* \right) |\varphi_{A,\gamma_A}\rangle\langle\varphi_{A,\gamma'_A}|. \quad (49)$$

Let the number of states in the block a be D and the degrees of freedom of one site be d . The number of states of the chain scales exponentially with the chain length, therefore the aim of the truncation is to keep such D' states that are presented

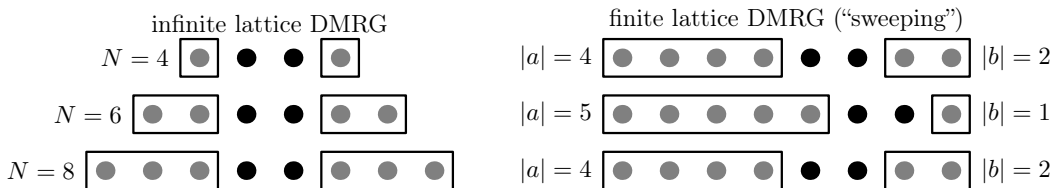


Figure 7: The infinite lattice algorithm builds up the chain. The finite lattice algorithm reloads and iterates the stored block states and block operators until the representation is converged enough.

with the highest weight in the subsystem \mathcal{A} . That is, using the decomposition (16), the eigenvectors with the largest $\omega_1, \dots, \omega_{D'}$ eigenvalues are arranged into the transformation matrix O_T , having size of $(D' \times Dd)$, by which the operators $O_{a'}$ acting on the new $a' = \{1, \dots, \ell, \ell + 1\}$ block are generated:

$$O_{a'} = O_T(O_a \otimes O_{\{\ell+1\}})O_T^\dagger \equiv O_T(O_{\mathcal{A}})O_T^\dagger, \quad (50)$$

where the size of O_a and $O_{\{\ell+1\}}$ are $(D \times D)$ and $(d \times d)$, respectively. Because of the incompleteness of the new basis,

$$\sum_{\gamma_{a'}=1}^{D'} |\psi_{a', \gamma_{a'}}\rangle \langle \psi_{a', \gamma_{a'}}| \neq \mathbf{I}, \quad (51)$$

truncation error arises in a renormalization step, which can be quantified as

$$\epsilon = 1 - \sum_{\gamma_{a'}=1}^{D'} \omega_{\gamma_{a'}}. \quad (52)$$

The next step of the algorithm is started with the relabelling $a' \rightarrow a$.

To build up the chain four one-site states are obtained at the beginning. With the symmetric expansion of the left and right blocks, the DMRG steps are repeated until the demanded chain length is reached. This is the so-called *infinite lattice* DMRG algorithm, in which the data of blocks is stored in the machine in each step. After constructing the chain of length N , the *finite lattice* DMRG algorithm systematically resizes the blocks to iterate the states and lattice operators ("sweeping") as it is illustrated schematically in Figure 7.

A DMRG step can be considered as a *singular value decomposition* (SVD). In each renormalization step one can reshape the transformation operator O_T , which is of size $D' \times Dd$, to obtain d pieces of matrices \mathbf{A} each is of size $D' \times D$. If the chain is represented by these matrices, this is called an MPS type representation of the problem, which will be discussed in details in the following section. A chain of



Figure 8: Representation of the coefficient tensor c and the MPS matrices \mathbf{A} .

length N without truncation would be represented by matrices $\mathbf{A}_1, \dots, \mathbf{A}_N$ of size $(1 \times d), (d \times d^2), \dots, (d^{\frac{N}{2}-1} \times d^{\frac{N}{2}}), (d^{\frac{N}{2}} \times d^{\frac{N}{2}-1}), \dots, (d \times 1)$. However, the necessity of restriction of the Hilbert space to a submanifold accessible by MPS is obvious. That is, the number of the retained states is limited via truncation so the matrices \mathbf{A} are of size, e.g. $(1 \times d), (d \times d^2), (d^2 \times d^3), (d^3 \times D), (D \times D), \dots, (D \times d^3), \dots, (d \times 1)$ in practical calculations.

From this point of view one can say that the DMRG algorithm does the optimization of the MPS matrices, or in other words, DMRG is a variational method that uses ansatz of form MPS [33, 34]. The relation between DMRG and MPS are comprehensively detailed in reference [35], while in the next section only the fundamentals are discussed which are related to this thesis.

4 Matrix product state (MPS)

An arbitrary state vector expanded on the tensor product basis is written as

$$|\psi\rangle = \sum_{\gamma_1, \gamma_2, \dots} c_{\gamma_1, \gamma_2, \dots} |\varphi_{1, \gamma_1}\rangle \otimes |\varphi_{2, \gamma_2}\rangle \otimes \dots, \quad (53)$$

where the indices $\gamma_1, \gamma_2, \dots$ can attain d_1, d_2, \dots number of values (local degrees of freedom). The entries of the coefficient tensor $c \in \mathbb{C}^{d_1 \times d_2 \times \dots}$ scales exponentially with the chain of length N , thus the numerical treatment is infeasible even for not too large systems. A possible solution is to factorize the coefficient tensor into coefficient matrices as it is illustrated in figure 8. For this reason let us consider the reshaping $c_{\gamma_1, \gamma_2, \dots} = C_{(\gamma_1), (\gamma_2, \gamma_3, \dots)}^{[1]}$, and apply the singular value decomposition (16) on matrix $\mathbf{C}^{[1]} \in \mathbb{C}^{d_1 \times (d_2 \cdot d_3 \cdot \dots)}$ to get the form $\mathbf{C} = \mathbf{U} \mathbf{S} \mathbf{V}^\dagger$.

$$C_{(\gamma_1), (\gamma_2, \gamma_3, \dots)}^{[1]} = \sum_{\alpha_1} U_{(\gamma_1), \alpha_1}^{[1]} S_{\alpha_1, \alpha_1}^{[1]} (V^{[1]^\dagger})_{\alpha_1, (\gamma_2, \gamma_3, \dots)} \equiv \sum_{\alpha_1} A_{1, \gamma_1}^{\alpha_1} C_{(\alpha_1, \gamma_2), (\gamma_3, \dots)}^{[2]} \quad (54a)$$

In the second equation we merge the singular values s_{α_1} into $\mathbf{V}^{[1]^\dagger}$ to get $C^{[2]}$. Indices of physical relevance are the γ -s (e.g. projection of angular momentum or the occupation number of molecular orbitals) so they are called *physical indices*, while the α -s are the *virtual indices* appearing in the SVD. Accordingly, $\mathbf{U}^{[1]}$ should be represented as the collection of vectors \mathbf{A}_{1, γ_1} . In the next step the decomposition

is

$$C_{(\alpha_1, \gamma_2), (\gamma_3, \dots)}^{[2]} = \sum_{\alpha_2} U_{(\alpha_1, \gamma_2), \alpha_2}^{[2]} S_{\alpha_2, \alpha_2}^{[2]} (V^{[2]\dagger})_{\alpha_2, (\gamma_3, \dots)} \equiv \sum_{\alpha_1} A_{2, \gamma_2}^{\alpha_1 \alpha_2} C_{(\alpha_2, \gamma_3), (\gamma_4, \dots)}^{[3]}, \quad (54b)$$

where the matrices \mathbf{A}_{2, γ_2} correspond to the order-three tensor $U^{[2]}$. Continuing the decomposition until the end of the chain the MPS form of the state vector is

$$|\psi\rangle = \sum_{\gamma_1, \gamma_2, \dots, \gamma_N} \mathbf{A}_{1, \gamma_1} \mathbf{A}_{2, \gamma_2} \dots \mathbf{A}_{N, \gamma_N} |\varphi_{1, \gamma_1}\rangle \otimes |\varphi_{2, \gamma_2}\rangle \otimes \dots \otimes |\varphi_{N, \gamma_N}\rangle. \quad (55)$$

By this one can obtain the expectation value of an observable $O = O_1 \otimes O_2 \otimes \dots \otimes O_N$,

$$\begin{aligned} \langle \psi | O | \psi \rangle = & \\ & \sum_{\substack{\gamma'_N, \\ \gamma_N}} O_{N, \gamma'_N, \gamma_N} \mathbf{A}_{N, \gamma'_N}^\dagger \left(\dots \left(\sum_{\substack{\gamma'_2, \\ \gamma_2}} O_{2, \gamma'_2, \gamma_2} \mathbf{A}_{2, \gamma'_2}^\dagger \left(\sum_{\substack{\gamma'_1, \\ \gamma_1}} O_{1, \gamma'_1, \gamma_1} \mathbf{A}_{1, \gamma'_1}^\dagger \mathbf{A}_{1, \gamma_1} \right) \mathbf{A}_{2, \gamma_2} \right) \dots \right) \mathbf{A}_{N, \gamma_N}, \end{aligned} \quad (56)$$

where O_i is a linear operator of the Hilbert space assigned to the i -th site, and the matrix elements of it are $O_{i, \gamma'_i, \gamma_i} = \langle \varphi_{i, \gamma'_i} | O_i | \varphi_{i, \gamma_i} \rangle$. The density matrix of the pure system is

$$\begin{aligned} |\psi\rangle\langle\psi| = & \sum_{\substack{\gamma_1, \gamma_2, \dots, \gamma_N \\ \gamma'_1, \gamma'_2, \dots, \gamma'_N}} \mathbf{A}_{1, \gamma_1} \mathbf{A}_{2, \gamma_2} \dots \mathbf{A}_{N, \gamma_N} \mathbf{A}_{N, \gamma'_N}^\dagger \dots \mathbf{A}_{2, \gamma'_2}^\dagger \mathbf{A}_{1, \gamma'_1}^\dagger \times \\ & \times |\varphi_{1, \gamma_1}\rangle\langle\varphi_{1, \gamma'_1}| \otimes |\varphi_{2, \gamma_2}\rangle\langle\varphi_{2, \gamma'_2}| \otimes \dots \otimes |\varphi_{N, \gamma_N}\rangle\langle\varphi_{N, \gamma'_N}|. \end{aligned} \quad (57)$$

The DMRG state, according to (47), is represented by a order-four tensor, and the operators are matrices of size $(D_a \times D_a)$, $(d_{\{\ell+1\}} \times d_{\{\ell+1\}})$, $(d_{\{\ell+2\}} \times d_{\{\ell+2\}})$, $(D_b \times D_b)$. Therefore, the DMRG framework is an *operator-like* approach because the operators O_a (50) are renormalized during an iteration. While, in the MPS representation the site operators are of size $(d_j \times d_j)$ but N pieces of $D \times D'$ sized matrices are needed to construct the state with configuration $\gamma_1, \dots, \gamma_N$; for this reason this is a *state-like* approach. The graphical illustration of the two representations is in figure 9.

In case of spin models d is in order 1. To examine gapped models, in which block entropy and D saturate, chains with thousands of sites can be obtained. In critical models 20 – 50 thousand block states are need to be retained for the appropriate description, which limits the achievable chain length.

In the literature algorithms based on MPS representation are known as *post-DMRG* algorithms since DMRG provides the MPS from of the wave function. The

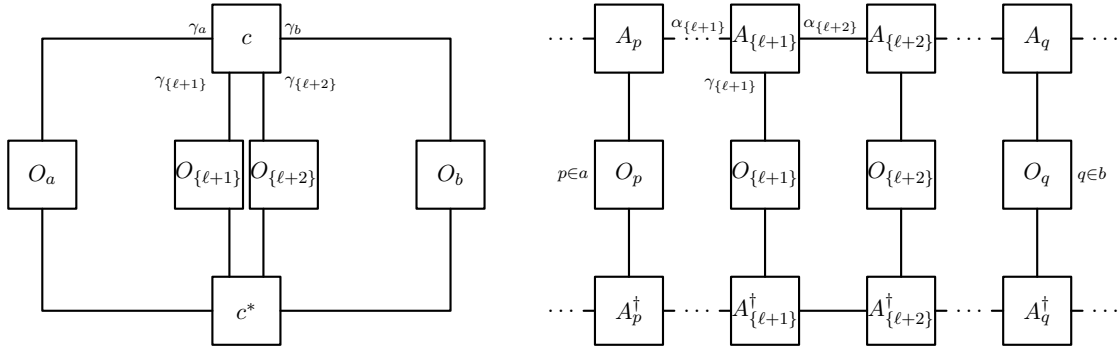


Figure 9: Calculation of expectation value with DMRG and MPS wave function. The contraction of two tensors are symbolized by joining the boxes with a line.

benefit of this framework manifests when expectation values of arbitrary operator combinations between different MPS-s, provided by independent DMRG calculations, are calculated. Such algorithms are being developed and optimized during my research work.

4.1 Valence bond solid

The importance of MPS formalism can be illustrated in a special, exactly solvable point of the bilinear-biquadratic model (4), named the AKLT point after Affleck, Lieb, Kennedy and Tasaki [36]. The ground state is the so-called valence bond solid (VBS) state, and the matrices \mathbf{A} are not obtained by SVD (54) but they can be calculated exactly for this particular problem.

One can prove the equivalence of the bilinear-biquadratic model (4) with the choice $\theta = \arctan \frac{1}{3}$ and a Hamilton operator which is the sum of projectors mapping onto the $S = 2$ subspace of two neighbouring spins [1]. The $S = 1$ state space is built up by basis vectors $|\varphi_{i,\pm\frac{1}{2}}\rangle$ representing spin-halves ($\dim \mathcal{H}_i = 2$). The antiferromagnetic ground state is constructed such a way that certain neighbouring spin-halves form singlet state, which can be interpreted as valence bonds:

$$\begin{array}{c}
 \text{end-spin} \curvearrowright \begin{array}{c} \text{singlet} \\ \bullet \text{---} \bullet \\ \text{---} \bullet \text{---} \bullet \end{array} \dots \\
 \mathcal{H} = \mathcal{H}_1 \otimes \mathcal{H}_2 \otimes \mathcal{H}_3 \otimes \mathcal{H}_4 \otimes \mathcal{H}_5 \otimes \dots \\
 |\tilde{\Psi}\rangle = |\varphi_1\rangle \otimes |\phi_{\{2,3\}}\rangle \otimes |\phi_{\{4,5\}}\rangle \otimes \dots
 \end{array} \tag{58}$$

The singlet states in the basis $\frac{1}{2} \otimes \frac{1}{2}$ are

$$|\phi_{\{i,i+1\}}\rangle = \sum_{\alpha_i, \alpha_{i+1} = -\frac{1}{2}, \frac{1}{2}} \phi_{\{i,i+1\}}^{\alpha_i \alpha_{i+1}} |\varphi_{i, \alpha_i}\rangle \otimes |\varphi_{i+1, \alpha_{i+1}}\rangle, \quad i = 2, 4, 6, \dots, \quad (59)$$

$$\phi_{\{i,i+1\}} = \begin{bmatrix} 0 & \frac{1}{\sqrt{2}} \\ -\frac{1}{\sqrt{2}} & 0 \end{bmatrix}.$$

We need a map that gives the state vector of the chain expanded on the triplet subspace $\{|\varphi_{\{i-1,i\},\gamma}\rangle\}_{\gamma=-1,0,1}$ with the restriction in the sum of the neighbouring spins-ones, which is $|\mathbf{S}_{\{i-1,i\}} + \mathbf{S}_{\{i+1,i+2\}}| < 2$ [1]. This is obtained by retaining only the triplet states of the spin- $\frac{1}{2}$ pairs in each bubble (seen in the figure of (58)), which are

$$|\psi_{\{i-1,i\},\gamma}\rangle = \sum_{\alpha_{i-1}, \alpha_i = -\frac{1}{2}, \frac{1}{2}} \psi_{\{i-1,i\},\gamma}^{\alpha_{i-1} \alpha_i} |\varphi_{i-1, \alpha_{i-1}}\rangle \otimes |\varphi_{i, \alpha_i}\rangle, \quad i = 2, 4, 6, \dots,$$

$$\boldsymbol{\psi}_{\{i-1,i\},-1} = \begin{bmatrix} 1 & 0 \\ 0 & 0 \end{bmatrix}, \quad \boldsymbol{\psi}_{\{i-1,i\},0} = \begin{bmatrix} 0 & \frac{1}{\sqrt{2}} \\ \frac{1}{\sqrt{2}} & 0 \end{bmatrix}, \quad \boldsymbol{\psi}_{\{i-1,i\},+1} = \begin{bmatrix} 0 & 0 \\ 0 & 1 \end{bmatrix}. \quad (60)$$

That is, applying the map

$$P_{\{i-1,i\},\gamma} : \mathcal{H}_{i-1} \otimes \mathcal{H}_i \rightarrow \mathcal{K}_{\{i-1,i\}} \quad (\dim \mathcal{K}_{\{i-1,i\}} = 3)$$

$$P_{\{i-1,i\}} = \sum_{\gamma=-1,0,1} P_{\{i-1,i\},\gamma} = \sum_{\gamma=-1,0,1} |\varphi_{\{i-1,i\},\gamma}\rangle \langle \psi_{\{i-1,i\},\gamma}|, \quad (61)$$

on the state vector $|\tilde{\Psi}\rangle$ in equation (58), then the ground state of the AKLT model is

$$|\Psi\rangle = \left(P_{\{1,2\}} \otimes P_{\{3,4\}} \otimes \dots \right) \left(|\varphi_{\{1\}}\rangle \otimes |\phi_{\{2,3\}}\rangle \otimes |\phi_{\{4,5\}}\rangle \otimes \dots \right). \quad (62)$$

Writing out the operation of P , using the formulas (59) and (60), finally relabelling as $\{i-1, i\} \rightarrow \frac{i}{2}$, the MPS form is obtained:

0.436	+	-	+	-
	0	0	0	0
0.218	0	+	0	-
	+	0	-	0
-0.218	+	0	0	-
	+	-	0	0
	0	0	+	-
$\approx 10^{-16}$	+	+	-	-
	+	-	-	+

Table 1: DMRG calculation for VBS state in the quantum number sector $S_{tot}^z = 0$ without truncation since $N = 4$. States obtained by exchanging $+$ \leftrightarrow $-$ are not listed, they have the same coefficient in the wave function.

$$\begin{aligned}
|\Psi\rangle &= \\
&\sum_{\substack{\gamma_{\{1,2\}}, \\ \gamma_{\{3,4\}}, \dots \\ = -1, 0, 1}} \sum_{\substack{\alpha_1, \alpha_2, \dots \\ = -\frac{1}{2}, \frac{1}{2}}} \underbrace{\varphi_{\{1\}}^{\alpha_1} \psi_{\{1,2\}, \gamma_{\{1,2\}}}^* \alpha_1 \alpha_2}_{\varphi_{\{1,2\}, \gamma_{\{1,2\}}}^{\alpha_1} \psi_{\{1,2\}, \gamma_{\{1,2\}}}^* \alpha_1 \alpha_2} \underbrace{\phi_{\{2,3\}}^{\alpha_2 \alpha_3} \psi_{\{3,4\}, \gamma_{\{3,4\}}}^* \alpha_3 \alpha_4}_{\phi_{\{2,3\}}^{\alpha_2 \alpha_3} \psi_{\{3,4\}, \gamma_{\{3,4\}}}^* \alpha_3 \alpha_4} \dots |\varphi_{\{1,2\}, \gamma_{\{1,2\}}}\rangle \otimes |\varphi_{\{3,4\}, \gamma_{\{3,4\}}}\rangle \dots = \\
&\sum_{\substack{\gamma_1, \gamma_2, \dots \\ = -1, 0, 1}} \sum_{\substack{\beta_1, \beta_2, \dots \\ = -\frac{1}{2}, \frac{1}{2}}} A_{1, \gamma_1}^{\beta_1} \quad A_{2, \gamma_2}^{\beta_1 \beta_2} \quad \dots \quad |\varphi_{1, \gamma_1}\rangle \otimes |\varphi_{2, \gamma_2}\rangle \dots = \\
&\sum_{\substack{\gamma_1, \gamma_2, \dots \\ = -1, 0, 1}} \mathbf{A}_{1, \gamma_1} \quad \mathbf{A}_{2, \gamma_2} \quad \dots \quad |\varphi_{1, \gamma_1}\rangle \otimes |\varphi_{2, \gamma_2}\rangle \dots
\end{aligned} \tag{63}$$

Except for the ends, three matrices are assigned to every sites, which are

$$\mathbf{A}_{i,-1} = \begin{bmatrix} 0 & 0 \\ -\frac{1}{\sqrt{2}} & 0 \end{bmatrix}, \quad \mathbf{A}_{i,0} = \begin{bmatrix} \frac{1}{2} & 0 \\ 0 & -\frac{1}{2} \end{bmatrix}, \quad \mathbf{A}_{i,+1} = \begin{bmatrix} 0 & \frac{1}{\sqrt{2}} \\ 0 & 0 \end{bmatrix}. \tag{64}$$

The matrices $\mathbf{A}_{i,\pm 1}$ are nilpotent, that is, components in which two $+1$ or two -1 are next to each other have zero coefficient in the expansion of MPS vector. Moreover, if one disregards the 0 index values in the non-zero terms of the expansion, then the $+1$ and -1 index values appear alternately, which is shown in the table 1. This Néel-type order is preserved in ground state and the 0 states can move freely, which indicates a *hidden topological* order, which can be characterized with

the expectation value of the *string operator* [37]:

$$g(i, j) = - \left\langle S_i^z \exp \left(i\pi \sum_{k=i+1}^{j-1} S_k^z \right) S_j^z \right\rangle. \quad (65)$$

In the VBS state the limit is non-vanishing, $g(|i-j| \rightarrow \infty) = \frac{4}{9}$, and in case of open boundary conditions the $S = \frac{1}{2}$ *end-spins*, emphasised in the figure of equation (58), lead to the fourfold degeneration of the ground state. Having this exactly solvable problem in the bilinear-biquadratic model (4) in hand, my first task was the implementation of this problem to have a reference point for the general MPS routines.

5 Results

In statistical physics for the description of the long-range order *correlation functions* are introduced, that is, correlations of observables (26) are examined in the function of real or momentum space distance.

In case of spin chains the correlation function of the spin projection operator S^z ,

$$C_{i|j}(\varrho_{ij}; S_i^z, S_j^z) = \langle S_i^z \otimes S_j^z \rangle - \langle S_i^z \rangle \langle S_j^z \rangle, \quad (66)$$

is commonly studied. Loosely speaking, this detects the relationship of sites i and j considering the projection of the spins. The long range behaviour of physical models having energy gap Δ between the ground state and the excited states can be characterized by the correlation length $\xi_c \propto \frac{1}{\Delta}$ as

$$C_{i|j}(\varrho_{ij}; S_i^z, S_j^z) \underset{\Delta \neq 0}{\propto} e^{-\frac{|i-j|}{\xi_c}}. \quad (67)$$

On the other hand, the energy of excited states in a critical system are infinitesimally close to the ground state energy in thermodynamic limit; the correlation function (66) decays not exponentially but algebraically (with power-law) with exponent η :

$$C_{i|j}(\varrho_{ij}; S_i^z, S_j^z) \underset{\Delta=0}{\propto} |i-j|^{-\eta}. \quad (68)$$

In section 2 the close relation of the correlations of observables and the mutual information w.r.t. a partition was discussed in details. In addition, from the definitions (38) and (26) one can derive the inequality [38, 39]

$$I_{i|j}(\varrho_{ij}) \geq \frac{C_{i|j}(\varrho_{ij}; O_i, O_j)^2}{2\|O_i\|_\infty^2 \|O_j\|_\infty^2}. \quad (69)$$

Supposing the same type of function (exponential or algebraic) for $I_{i|j}$ and $C_{i|j}$, then the exponent ($\frac{2}{\xi_c}$ or 2η) in $I_{i|j}$ is at least twice as big as that in the slowest decaying $C_{i|j}$ [39]. Moreover, analogous inequalities can be obtained for ξ -correlation functions and ξ -mutual informations.

Besides the expression (66) many other correlation functions with physically relevant operator combinations could have expressive meaning, so the *generalized correlation functions* are useful to study [39]. Therefore, let us introduce linear operators in the d dimensional Hilbert space \mathcal{H} which bring the basis vectors into each other:

$$T_{\gamma'\gamma}|\varphi_\gamma\rangle = |\varphi_{\gamma'}\rangle, \quad T_{\gamma'\gamma}^{\alpha'\alpha} = \delta_{\gamma'\alpha'}\delta_{\gamma\alpha}. \quad (70)$$

There are d^2 transition operators $T_{\gamma'\gamma} = |\varphi_{\gamma'}\rangle\langle\varphi_\gamma|$, which can be represented as $d \times d$ matrices each with one non-zero entry. They span the space $\text{Lin } \mathcal{H}$, so arbitrary operator of observable can be expanded in it. For example, for spin-halves $S_i^z = -\frac{1}{2}T_{i,\downarrow\downarrow} + \frac{1}{2}T_{i,\uparrow\uparrow}$. The expectation values of operators defined in (70) are the matrix elements of the one-site state ϱ_i . The two-site correlation function of operators T_i, T_j can be expressed with the entries of the one- and two-site density matrices:

$$C(\varrho_{i|j}, T_{i,\gamma'_i\gamma_i}, T_{j,\gamma'_j\gamma_j}) = \langle T_{i,\gamma'_i\gamma_i} \otimes T_{j,\gamma'_j\gamma_j} \rangle - \langle T_{i,\gamma'_i\gamma_i} \rangle \langle T_{j,\gamma'_j\gamma_j} \rangle = \varrho_{ij}^{\gamma_i\gamma'_i, \gamma_j\gamma'_j} - \varrho_i^{\gamma_i\gamma'_i} \cdot \varrho_j^{\gamma_j\gamma'_j}. \quad (71)$$

Since inequality (69) is valid for correlation functions of arbitrary operators O_i, O_j , then it is also valid for that of operators T_i, T_j . Similarly, ξ -correlation functions of transition operators can be introduced for a multipartite system.

Let us consider a chain of length N , and extract a tripartite system $\{a, b, c\}$ from the entire system $L = \{1, 2, \dots, N\}$ as

$$\begin{aligned} a(l) &= \frac{N}{2} - l, \\ b(l) &= \frac{N}{2}, \\ c(l) &= \frac{N}{2} + l. \end{aligned} \quad (72)$$

That is, the middle elementary subsystem b is fixed, and symmetrically further and further sites are chosen for elementary subsystems a and c by the increment of $l = 1, 2, \dots$. The construction and the partitioning is shown in figure 10. Consequently, ξ -correlation functions (26) and ξ -mutual information (38) for the states ϱ_{abc} are single-variable (l) functions.

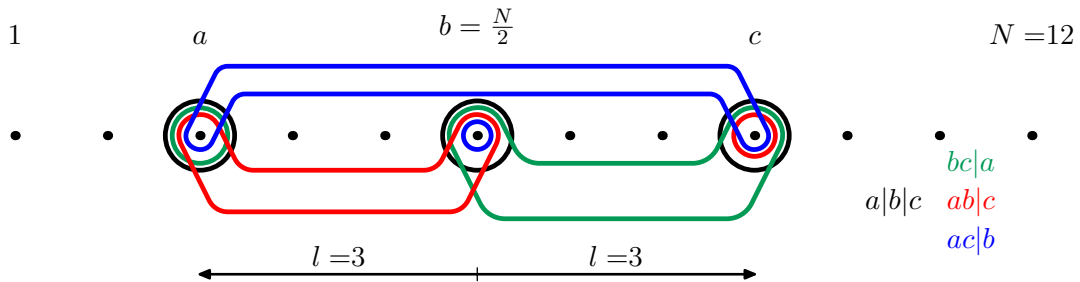


Figure 10: The tripartite system $\{a, b, c\} \subset L$ in the function of l and its non-trivial partitions illustrated for $N = 12$.

In section 2.4.1 the elementary subsystems were considered to be of equal role. Now, due to the geometry of (72), the elementary subsystems are *not of equal role* and the same holds for the different partitions of the same shape.

Considering the tripartite system (72) for a spin- $\frac{1}{2}$ model there are $4 \cdot 4 \cdot 4 = 64$ possible combinations of transition operators. However, the state vector is obtained by a DMRG calculation which is performed in a given total spin projection S_{tot}^z sector. Therefore, the expectation value is zero if an operator combination brings the state vector to an other sector, that is, it does not commute with the symmetry operator. Consequently, there are 20 combinations left. In addition, if we take into account that the role of subsystems a and c are the same, than there are 12 combinations to examine.

5.1 Spin-half J_1 - J_2 model

In the following, the illustration of the aforementioned notions is given using the model (3).

5.1.1 Majumdar–Ghosh model: $J_2 = \frac{1}{2}J_1$

The ground state of the spin-half J_1 - J_2 Heisenberg model (3) can be dimerized, as it was mentioned in the introduction. More precisely, it is dimerized when $\frac{J_2}{J_1} > 0.241$ [1]. Additionally, it is exactly solvable if $J_2 = \frac{1}{2}J_1$, and then the ground state is totally dimerized: the state vector is the tensor product of singlets $|\phi_{\{i,i+1\}}\rangle$ (59),

$$|\psi\rangle = |\phi_{\{1,2\}}\rangle \otimes |\phi_{\{3,4\}}\rangle \otimes \dots, \quad (73)$$

and only the energy of the singlet bond $\varepsilon_s = -\frac{3}{4}$ determines the total energy $\varepsilon = \frac{N}{2}\varepsilon_s$.

In this special case the graphs of pair correlations and block entropy, in figure 11, is easily understandable by the cutting of singlet bonds. The state of the

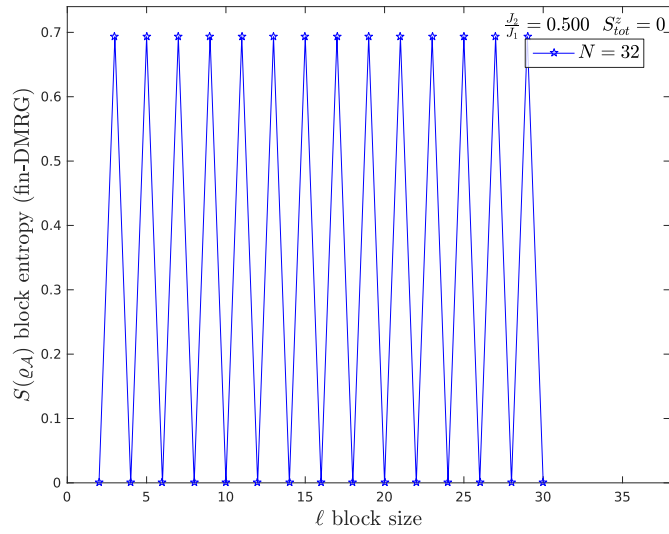
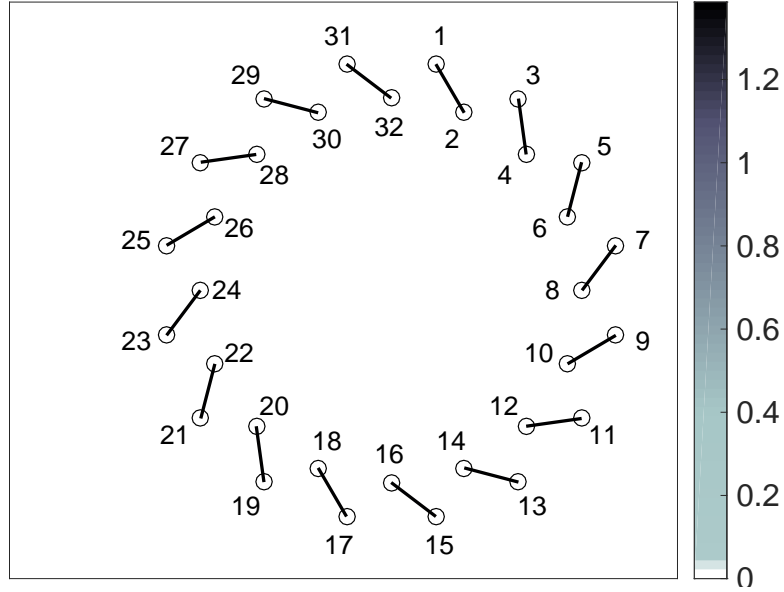


Figure 11: The ground state of the Majumdar–Ghosh model is totally dimerized, so pair correlation (pairwise mutual information) $I_{i|j}$ ($i, j \in L$) and the block entropy $S(\rho_{\mathcal{A}})$ ($|\mathcal{A}| = \ell$) have an extreme characteristic.

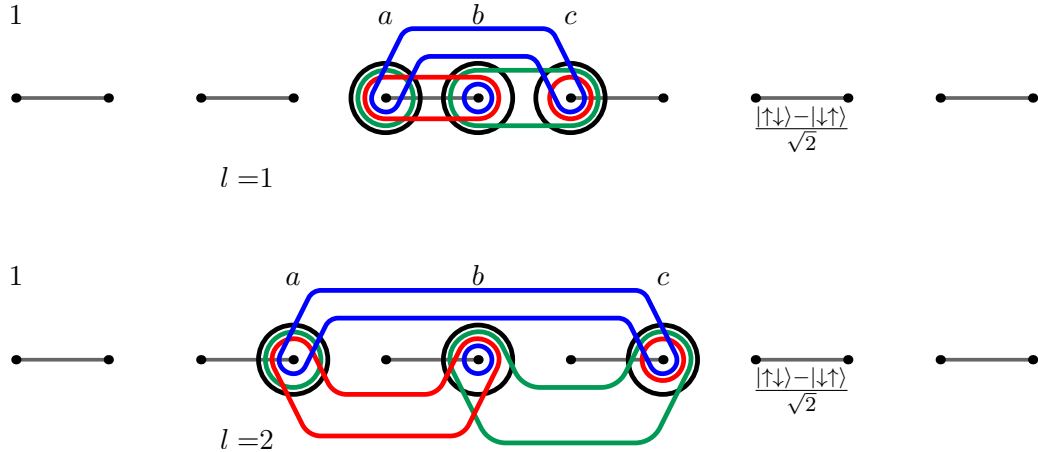


Figure 12: The non-trivial partitions of tripartite system $\{a, b, c\} \subset L$ on the totally dimerized chain for $l = 1$ and $l = 2$.

tripartite system of which geometry was described in the previous section is $\varrho_{abc} = \text{Tr}_{L \setminus \{a, b, c\}}(\varrho)$. One can apply the Schmidt decomposition (16) to the singlet bond which tells us that $\text{Tr}_1 |\phi_{\{1,2\}\rangle}\langle\phi_{\{1,2\}}| \cong \text{Tr}_2 |\phi_{\{1,2\}\rangle}\langle\phi_{\{1,2\}}|$ and the entropy of the one-site states is

$$S_a = S_b = S_c = \ln 2 \quad (74)$$

for all l . (If it is not misleading, the notations $S_a := S(\varrho_a)$ or $I_{a|c} := I_{a|c}(\varrho_{abc})$ are used.) If the sites are directly next to each other ($l = 1$), then one pair certainly forms a singlet bond, let us say a and b (see figure 12). This leads to

$$\begin{aligned} S_{ab} &= 0, & S_{ac} &= S_{bc} = 2 \ln 2, \\ S_{abc} &= \ln 2, \end{aligned}$$

because of the additivity of von Neumann entropy. This means that the entropy of a subsystem is as many times $\ln 2$ as many bonds are cut (partial trace applied on a singlet state) to obtain this system from the N -partite system. For the configuration of $l = 1$ the mutual informations (38) are

$$\begin{aligned} I_{a|b} &= 2 \ln 2, & I_{a|c} &= I_{b|c} = 0, \\ I_{ab|c} &= 0, & I_{ac|b} &= I_{cb|a} = 2 \ln 2, \\ I_{a|b|c} &= 2 \ln 2. \end{aligned}$$

However, for $l > 1$ each picked site is “contained” in a different singlet, as it is presented in the bottom part of figure 12. That is, as many cuts are needed as many subsystems we have. For this reason all further mutual informations of tripartite system $\{a, b, c\}$ are zero.

With these exactly calculated measures in hand one can check the general formula

$$I_{i|j|k} - I_{ij|k} = I_{i|j}, \quad (75)$$

which follows easily from the definition (38).

The oscillation of the block entropy can be explained similarly. The state of block \mathcal{A} containing even number of lattice sites is uncorrelated, while that containing odd number of sites is correlated with the complement (with other words, system L is correlated w.r.t. the partition $\mathcal{A}|\mathcal{B}$):

$$\begin{aligned} \varrho_{\{1,\dots,2k\}} &= |\phi_{\{1,2\}}\rangle\langle\phi_{\{1,2\}}| \otimes \dots \otimes |\phi_{\{2k-1,2k\}}\rangle\langle\phi_{\{2k-1,2k\}}| \\ \varrho_{\{1,\dots,2k+1\}} &= \varrho_{\{1,\dots,2k\}} \otimes \text{Tr}_{2k+2} |\phi_{\{2k+1,2k+2\}}\rangle\langle\phi_{\{2k+1,2k+2\}}| \end{aligned} \quad (76)$$

That is, the block entropy oscillates between $S(\varrho_{\{1,\dots,2k\}}) = 0$ and $S(\varrho_{\{1,\dots,2k+1\}}) = \ln 2$ along the chain as shown in figure 11.

The ξ -mutual informations (38), depending only on the state, were discussed so far for this model. It is easy to see that every ξ -correlation functions (26) are zero if $l > 1$, and also zero if it is taken w.r.t. $ab|c$ for $l = 1$.

5.1.2 Nearest neighbour interaction: $J_2 = 0$

The well-known antiferromagnetic Heisenberg chain is obtained by switching off the next nearest neighbour interaction in the model (3). The system is critical, long-range correlations occur, which can be seen in figure 13. The low-energy dispersion relation is $\varepsilon(k) = J_1 \frac{\pi}{2} |\sin k|$, that is, there are soft modes at $k = 0, \pi$ resulting two-site periodicity in real space quantities. One can prove that the behaviour of the block entropy for critical systems is

$$S_{\mathcal{A}}(\ell) \propto \ln \left[\frac{2N}{\pi} \sin \left(\frac{\pi \ell}{N} \right) \right], \quad (77)$$

which is now modulated by two-site oscillations [40, 7].

The correlation functions (66) exhibit power-law decay with exponent $\eta = 1$, but at higher l distances the *surface exponent* ($\eta_s \approx 2$) can be observed for the partition $a|c$, which is shown in figure 14. The distance of $a(l)$ and $c(l)$ is increasing by two in the term of l , that is, quantities w.r.t. partition $a|c$ and $ac|b$ do not exhibit that periodicity. A DMRG calculation illustrates the lack of tripartite S^z correlation in the table 2. A spin configuration and its flipped pair has the same coefficient in the wave function, therefore the expectation value of products of odd S^z operators is zero. Consequently, the corresponding correlation functions vanish, they are in the order of numerical precision, as it is in the second graph in figure 14.

The inequality (69) is probed by the correlation functions of transition operators in figure 15. Numerical equality is found for some operator combinations.

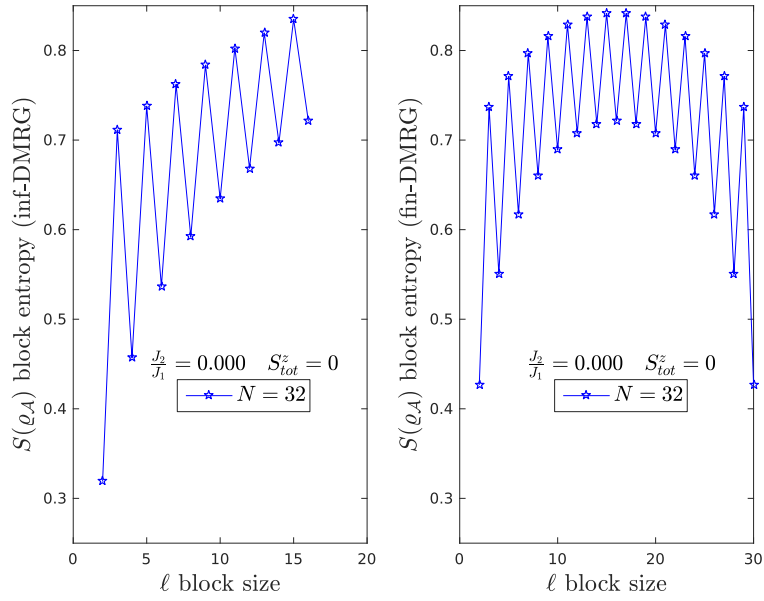
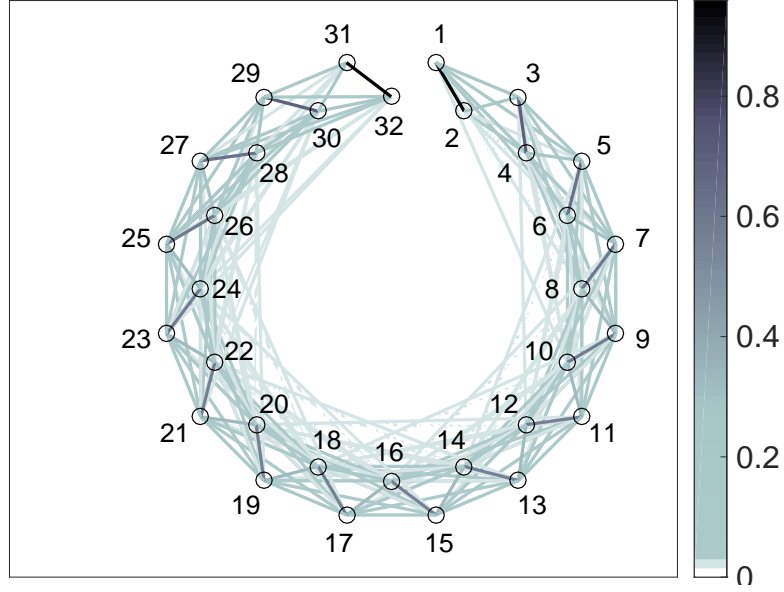


Figure 13: The pairwise mutual information clearly shows the long-range correlation in the $S = \frac{1}{2}$ Heisenberg model. The characteristics of the block entropy, obtained via infinite and finite lattice DMRG algorithm, is typical for critical systems.

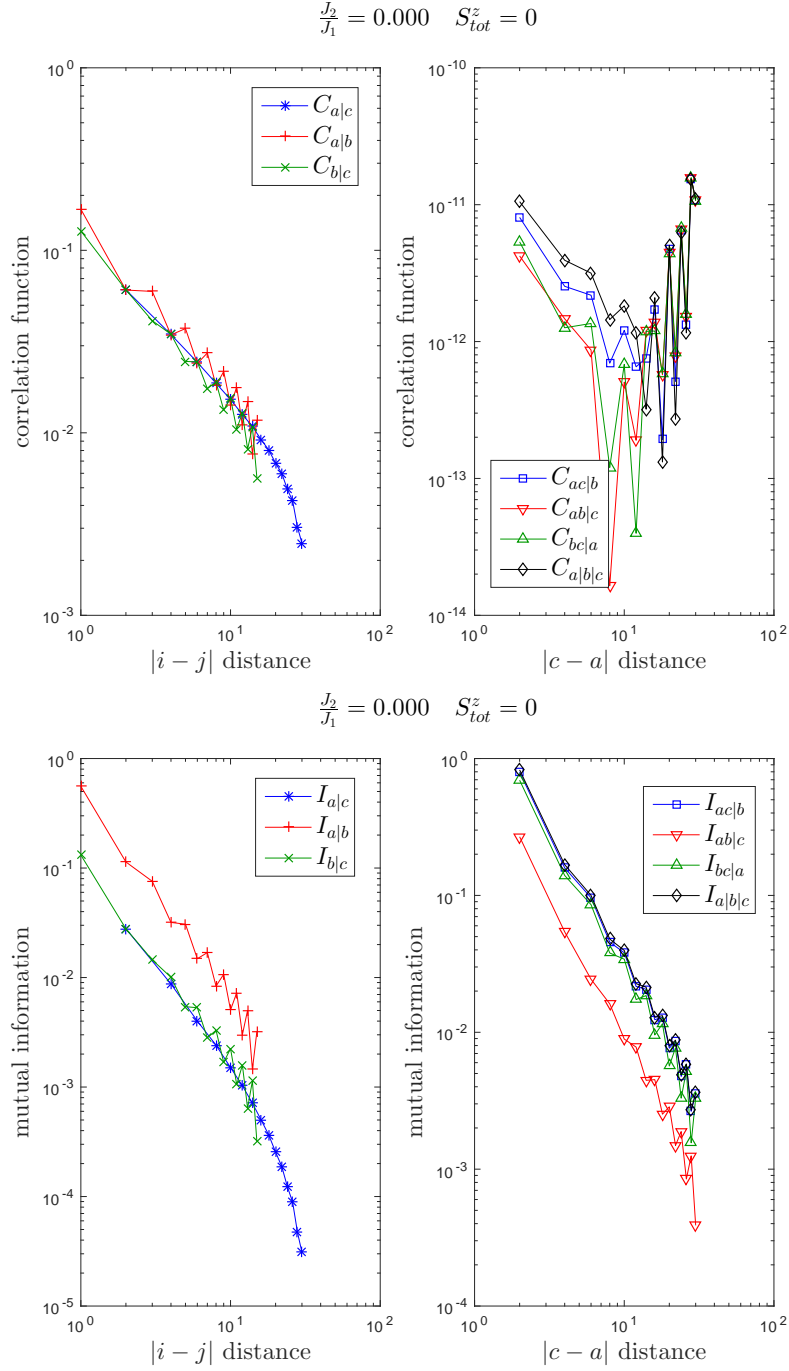


Figure 14: Correlation functions and mutual informations of the $S = \frac{1}{2}$ Heisenberg model. The tolerance of the diagonalization of the Hamilton operator is in the order of 10^{-9} , so for tripartite state the S^z operators are considered to be uncorrelated because the correlation functions are below this tolerance.

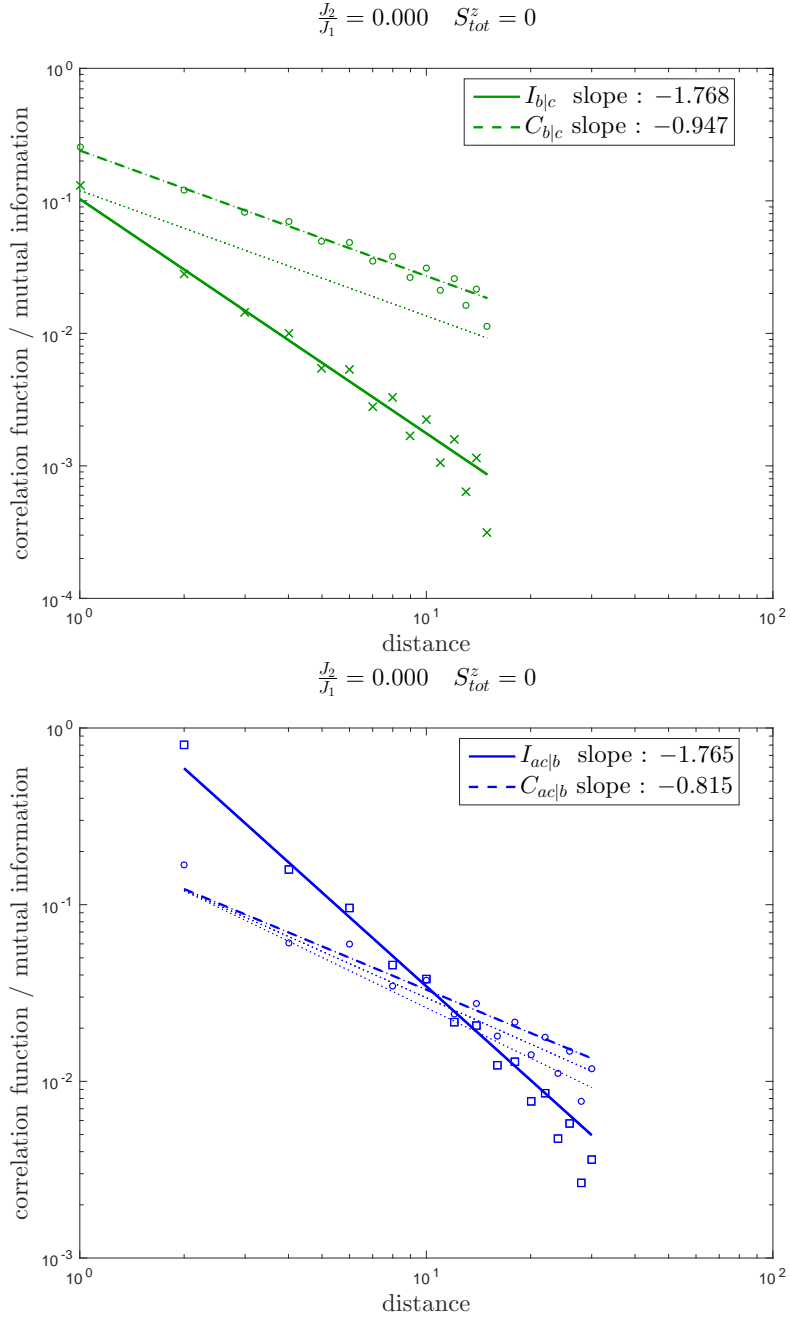


Figure 15: Fitting of mutual information and the slowest correlation function w.r.t. a given partition in the spin-half Heisenberg model. The slope of other correlation functions is plotted by dashed line.

0.558	$ \uparrow\downarrow\uparrow\downarrow\rangle$
0.558	$ \downarrow\uparrow\downarrow\uparrow\rangle$
-0.149	$ \uparrow\uparrow\downarrow\downarrow\rangle$
-0.149	$ \downarrow\downarrow\uparrow\uparrow\rangle$
-0.408	$ \uparrow\downarrow\downarrow\uparrow\rangle$
-0.408	$ \downarrow\uparrow\uparrow\downarrow\rangle$

Table 2: Demonstrative DMRG calculation in the subspace $S_{tot}^z = 0$ for $S = \frac{1}{2}$ Heisenberg chain of length $N = 4$.

5.2 Bilinear-biquadratic model

Special points and regions of the phase space of the model (4), illustrated in figure 2, is examined in the following.

5.2.1 Valence bond solid (VBS): $\theta = \arctan \frac{1}{3}$

The model is gapped so the correlation length is finite as the block entropy and mutual information show in figure 16. When the chain is built up by the infinite algorithm, the block entropy falls and saturates after only a few sites; this indicates the shortness of the correlation length. One can understand the plateau of the block entropy considering the diagram in equation (58). Every neighbouring sites are joint by a singlet bond in the ground state of AKLT model, which was discussed in section 4.1. If the chain is cut into two anywhere in the bulk, roughly speaking, singlet bond is cut, then each of the two subsystems has approximately the entropy of a traced singlet bond $\ln 2$.

The AKLT model is illustrative to study because the correlation functions are purely exponential with correlation length $\frac{1}{\xi_c} = \ln 3 \approx 1.099$ [41]. This results in the clear observation of the factor two between the slowest correlation function and mutual information [39]. In addition, with the help of tripartite measures we demonstrate the effect of one characteristic length in this gapped system. Mutual informations, in the function of the shortest distance between subsystems, decay with the same exponent ξ_c ; an example is given in figure 17. For every distance l the tripartite mutual informations are approximately equal, $I_{ac|b} = I_{ab|c} = I_{bc|a} = I_{a|b|c}$, which is the result of the short correlation length. In this model the system $\{a, b, c\}$ is not sensitive to the partitioning in this sense.

According to figure 2, being in the same (Haldane) phase, the AKLT model can be continuously transformed without closing the gap into the $\theta = 0$ Heisenberg model, which is studied in the following section.

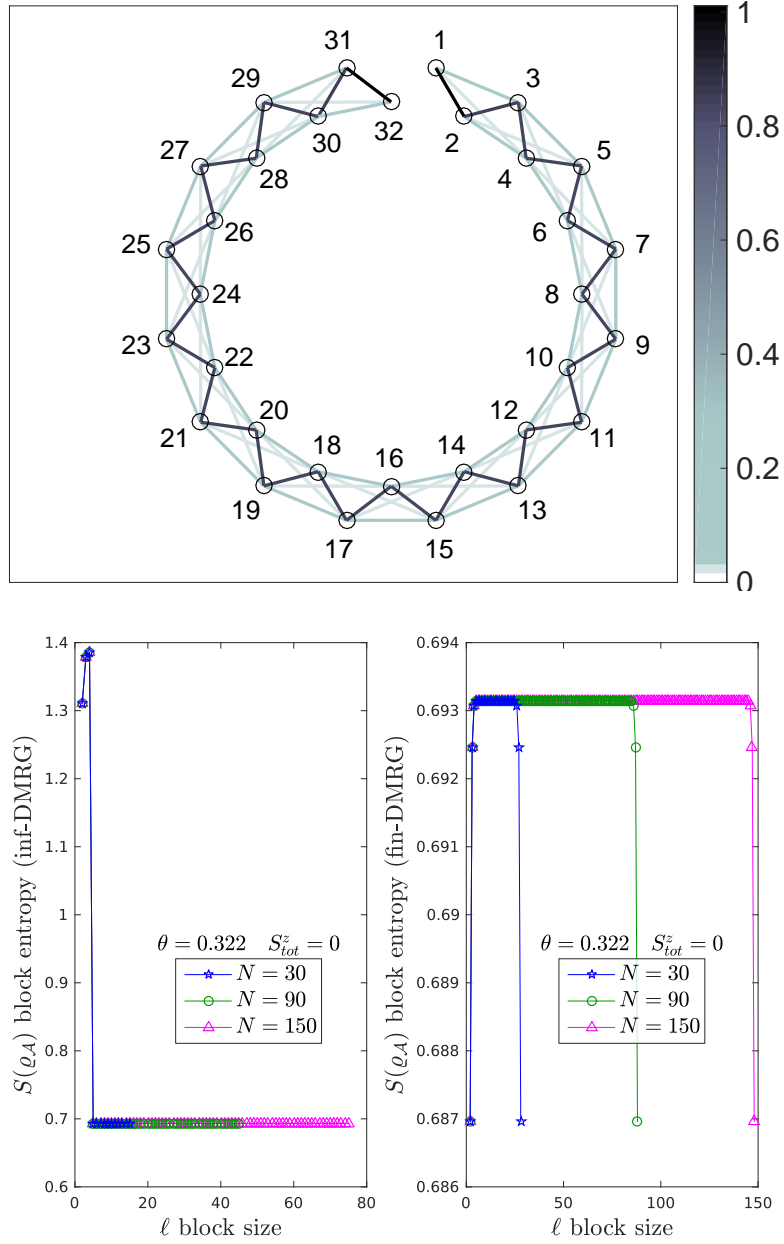
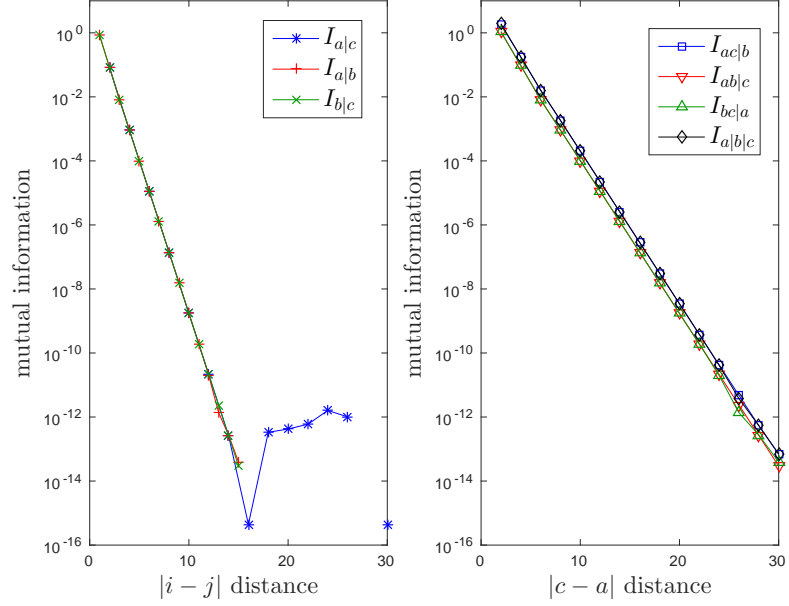


Figure 16: The VBS model has short correlation length, which is shown by the pairwise mutual information and the block entropy (obtained by infinite and finite DMRG algorithm).

$$\theta = 0.322 \quad S_{tot}^z = 0$$



$$\theta = 0.322 \quad S_{tot}^z = 0$$

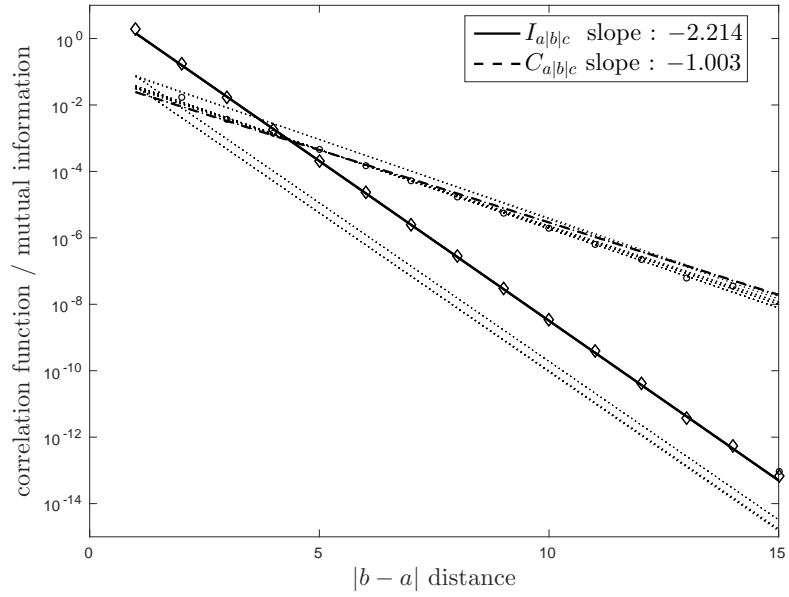


Figure 17: The purely exponential decays of mutual informations in VBS model, and the examination of the inequality (69).

5.2.2 Heisenberg model: $\theta = 0$

The correlation length in the $S = 1$ Heisenberg model is $\xi_c \approx 6.03$, which is longer than that of the VBS model. This leads to that the block entropy obtained by infinite lattice algorithm (in figure 18) increases until a critical block size ($\ell \approx 50$), which is larger than that of VBS model. Also, the graph of pairwise mutual information confirms the increased correlations in the chain.

In the figure 19 two- and four-site measures are examined. The bipartite system $\{a, c\}$ is obtained from the tripartite case (72), indicated in figure 10, that is, the distance between a and c increases by two. In case of the fourpartite system $\{a', b', c', d'\}$ there is no fixed site. They are symmetric to the point $\frac{N}{2} + \frac{1}{2}$ and the distance between the neighbouring sites is $l = 1, 3, 5, \dots$, that is,

$$\begin{aligned} a'(l) &= \frac{N+1}{2} - \frac{3}{2}l, \\ b'(l) &= \frac{N+1}{2} - \frac{1}{2}l, \\ c'(l) &= \frac{N+1}{2} + \frac{1}{2}l, \\ d'(l) &= \frac{N+1}{2} + \frac{3}{2}l. \end{aligned} \tag{78}$$

Due to the topological properties of the Haldane phase one can observe the *end-spin correlation*. The expectation value of the spin projection, presented in the third plot of figure 19, in the bulk tends to zero. However, the DMRG calculation is restricted to the $S_{tot}^z = 0$ subspace, that is why the spin projection increases in absolute value towards the surface. In the first plot of figure 19 the two-site S^z correlation function decays exponentially as expected, but tending towards the surface it increases with the same exponent for short chains. For longer chains the end-spin correlation dies out because of the finite correlation length. Mutual informations are also presented to show the equality in (69) for the bipartite S^z correlation function. Fourpartite quantities are also presented in figure 19. If elementary subsystems a' and d' are packed into one subsystem, than the end-spin correlation cannot be observed, that is, the $a'd'|b'c'$ -correlation functions and $a'd'|b'c'$ -mutual information decays until the end of the chain. Contrary, quantities w.r.t. partition $a'c'|b'd'$ shows the end-spin correlation.

5.2.3 Edges of the Haldane phase: $\theta = \pm\frac{\pi}{4}$

The gap of the Haldane phase is closed at $\theta = \pm\frac{\pi}{4}$, so in these points the models are critical but one can observe a difference in the oscillation of the block entropies,

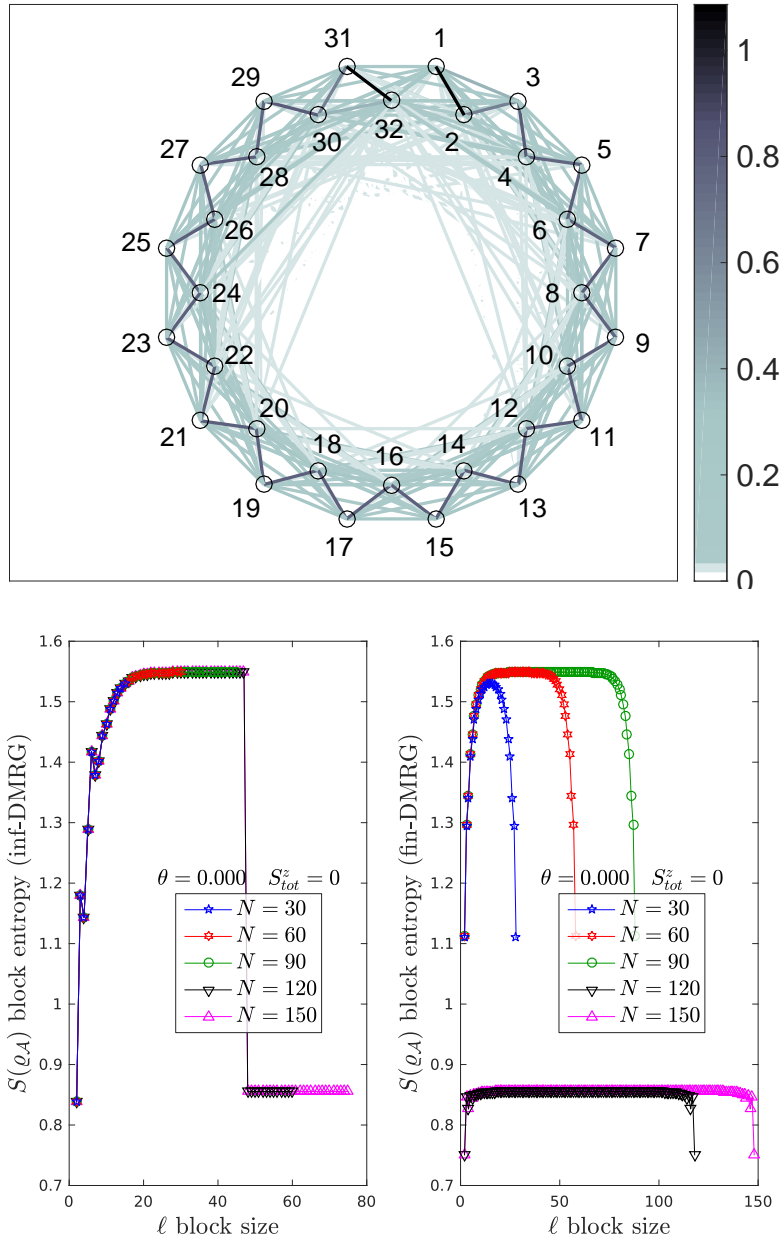


Figure 18: The pairwise mutual information and the block entropy for $S = 1$ Heisenberg model.

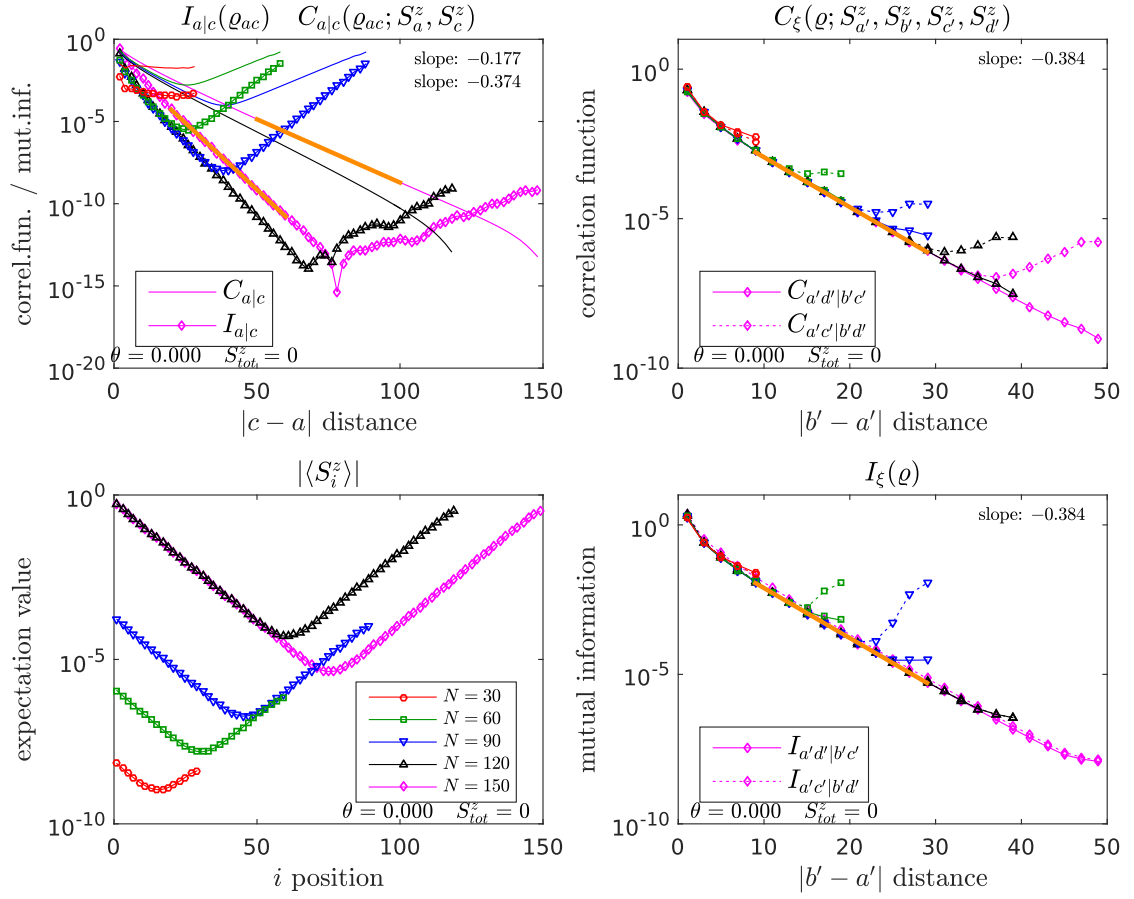


Figure 19: End-spin correlation in spin-one Heisenberg model.

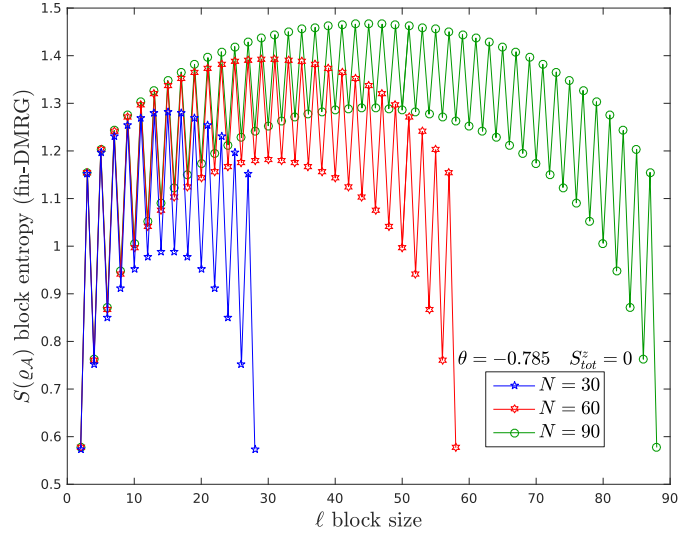
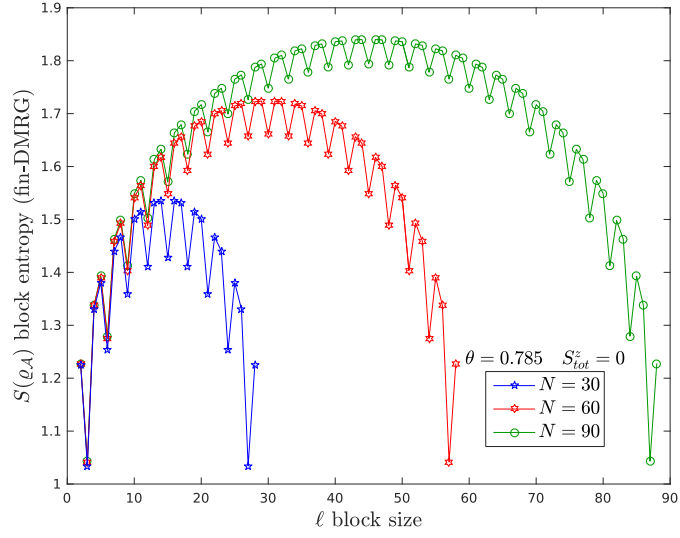


Figure 20: Block entropy of the “apparently trimerized” ($\theta = +\frac{\pi}{4}$) and “apparently dimerized” ($\theta = -\frac{\pi}{4}$) phase obtained by the finite lattice DMRG algorithm.

shown in figure 20. The Lai–Sutherland model, at $\theta = +\frac{\pi}{4}$, is integrable, and it turns out that the soft modes are at $k = 0, \pm\frac{2\pi}{3}$ in momentum space, which leads to a threefold periodicity in the block entropy. The region between ferromagnetic and Haldane phase shows similar properties, thus this is called *apparently trimerized* phase [42]. At $\theta = -\frac{\pi}{4}$ the model is also integrable, and it exhibits soft modes at $k = 0, \pi$, so twofold jumps can be seen in the block entropy. Therefore, this model, called Takhtajan–Babujian model, is said to be *apparently dimerized* [43].

The translational symmetry is not broken, hence the “apparently” adverb only refers to the finite-size effect. In thermodynamic limit ($N \rightarrow \infty$) the oscillations disappear in the block entropy, correlation functions and mutual informations. Calculations for longer chains are needed for the observation of this behaviour.

5.2.4 In the dimerized phase: $\theta = -\frac{\pi}{2}$

Leaving the Haldane phase in negative direction the *massively dimerized* phase can be found. At $\theta = -\frac{\pi}{2}$ the Hamilton operator (4) can be mapped onto the nine-state quantum Potts model, which provides an exact solution for the ground state [43].

As a result of the spontaneous breaking of the translational symmetry twofold periodicity appears in the block entropy, seen at the bottom of figure 21, which do not disappear in the thermodynamic limit. Having a gapped system in hand, for longer chains the envelope of the block entropy saturates, although the oscillations still occurs. Since the role of a and c is the same, as it was discussed around (72), mutual informations w.r.t. partitions $a|b$ and $b|c$ are on an equal footing. The oscillations in the decays are just shifted by one site, which can be seen at the top of figure 21. The same holds for partitions $ab|c$ and $bc|a$.

5.2.5 Spin nematic phase: $\theta \searrow -\frac{3\pi}{4}$

While the properties of the aforementioned phases are well established, there is a region in the phase diagram on which there has been long debate in the literature [44, 45, 46].

In the diagrams of figure 2 a possible phase, referred to as *spin nematic phase*, is depicted between the ferromagnetic and dimerized phase. In the dimerized phase the translational, in the ferromagnetic phase the $SU(2)$ symmetry is broken spontaneously. However, these symmetries are largely unrelated, and there seems to be no constraint which tells that the two transitions occur at the same point. According to the assumption of Chubukov, the gap could vanish and reopen at θ_c before the point $\theta = -\frac{3\pi}{4}$, resulting in a non-dimerized phase [47]. An other possibility is, instead of reopening, a critical region is sandwiched between the dimerized and ferromagnetic phases; or there is no intermediate phase. The three

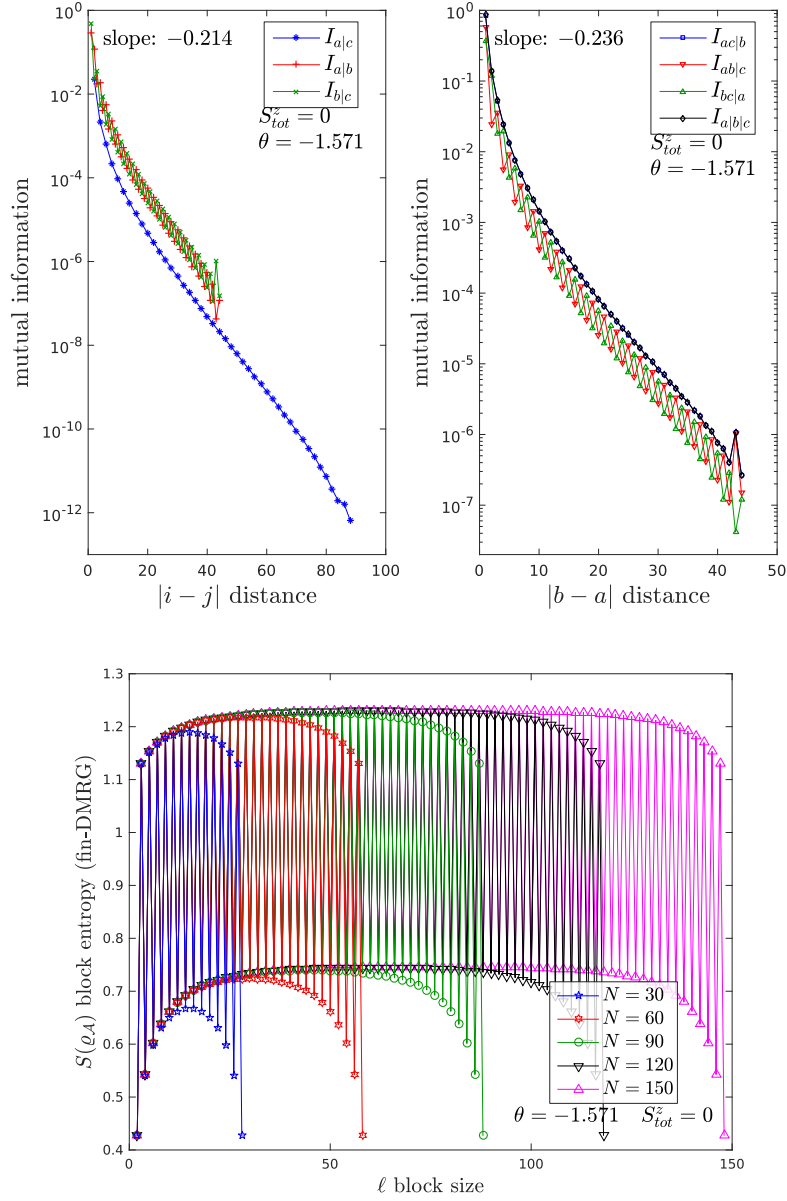


Figure 21: The mutual informations and the block entropy in the massively dimerized phase at $\theta = -\frac{\pi}{2}$.

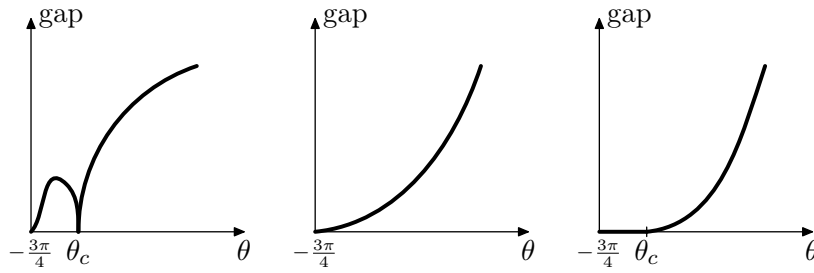


Figure 22: The energy gap according to the three possible ideas in the bilinear-biquadratic model around $\theta = -\frac{3\pi}{4}$ [48].

idea is illustrated in figure 22.

Block entropy obtained by DMRG calculation can be seen in figure 23. Longer chains and more block states are needed in our calculations in order to decide whether this region is gapped or not.

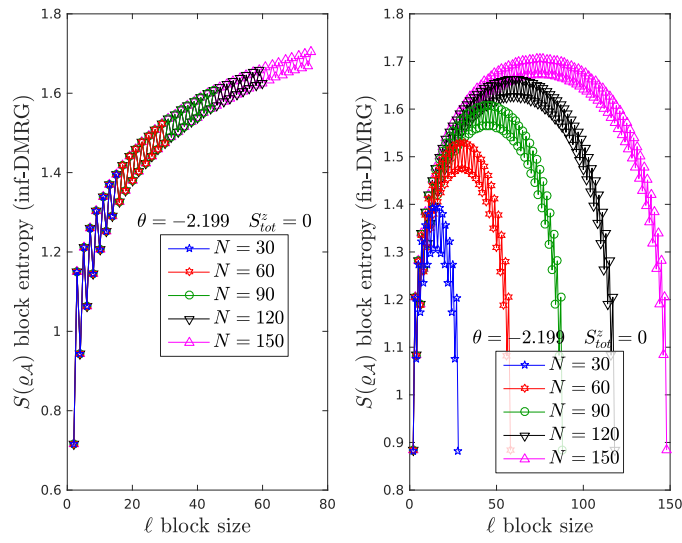


Figure 23: Block entropy for $\theta = -0.7\pi$ in the bilinear-biquadratic model. Going closer to the ferromagnetic phase, it is more difficult to decide whether the phase is gapped or not.

6 Summary

In my thesis I studied one-dimensional strongly correlated systems. This topic is of central importance in the field of quantum statistical physics, since several paradigmatic examples of exotic quantum phases can be observed even in one-dimensional systems. For the calculations I used the BUDAPEST-QC-DMRG implementation [49, 50], for which I developed MPS-based algorithms for the calculations of, for example, reduced density matrices or expectation values of arbitrary operators. In my investigations the main tool was the theory of multipartite correlations. For this I also implemented the lattice-theoretical structures encoding different kinds of multipartite correlations.

I have studied the multipartite correlations in the J_1 - J_2 Heisenberg model and the bilinear-biquadratic model. I determined the decays of ξ -mutual informations and ξ -correlation functions for different parameters of these models. In the Majumdar-Gosh case of the J_1 - J_2 Heisenberg model the totally dimerized ground state served as an illustrative example for the particular case when the multipartite correlations are built up from bipartite ones. Also the AKLT case of the bilinear-biquadratic model served as paradigmatic example of the MPS.

The numerical and theoretical methods I have learned during the preparation of my MSc thesis represent a versatile toolbox for the investigation of strongly correlated systems, therefore a wide range of possibilities opens for me in further research. I plan to investigate the multipartite correlations of chains exhibiting topological phases. Also, the two-site correlations show cluster structure in the $SU(N)$ Hubbard model (ultracold atomic systems), here I plan to investigate the multipartite correlations for the adequate analysis. I also plan to investigate the multipartite entanglement of two-dimensional electronic systems such as graphene nanoribbons and nanoflakes.

Acknowledgements

I would like to express my sincere gratitude to my advisers. It is a pleasure to thank *Dr. Örs Legeza* for his supervising and guidance helped me in all the time of research. I would like to extend my gratitude to *Dr. Szilárd Szalay* for steering me in the right direction with his passion for research. This work would not have been possible without the flexible and frequent discussions with them held in lighthearted atmosphere.

Useful discussions on numerical methods and tricks with *Dr. Gergely Barcza* and *Tamás Mosoni* are gratefully acknowledged.

My research was supported by the *Hungarian Scientific Research Fund* (project IDs: OTKANN110360, OTKAK120569) and the “*Lendület*” program (project ID: 81010-00) of the Hungarian Academy of Sciences.

My sincere thanks also goes to *Dr. Nguyen Quang Chinh* for introducing me to the scientific research during my early years in the university.

I would like to thank *Dávid Hegedüs* and *Kristóf Rozgonyi* friends of mine for all the fun we have had and their continuous encouragement throughout our bachelor and master studies.

Last but not least, I am grateful to *my parents* for their everlasting patience, support and love.

References

- [1] Sólyom, J. *Fundamentals of the Physics of Solids, Vol. 1, Structure and Dynamics* (Springer, 2007). URL <http://www.springer.com/materials/book/978-3-540-72599-2>.
- [2] Horodecki, R., Horodecki, P., Horodecki, M. & Horodecki, K. Quantum entanglement. *Rev. Mod. Phys.* **81**, 865–942 (2009).
- [3] Amico, L., Fazio, R., Osterloh, A. & Vedral, V. Entanglement in many-body systems. *Rev. Mod. Phys.* **80**, 517–576 (2008). URL <http://link.aps.org/doi/10.1103/RevModPhys.80.517>.
- [4] Buyers, W. J. L. *et al.* Experimental evidence for the haldane gap in a spin-1 nearly isotropic, antiferromagnetic chain. *Phys. Rev. Lett.* **56**, 371–374 (1986). URL <http://link.aps.org/doi/10.1103/PhysRevLett.56.371>.
- [5] Fazekas, P. *Lecture Notes on Electron Correlation and Magnetism (Series in Modern Condensed Matter Physics, Vol. 5)* (World Scientific Pub Co Inc, 1999).
- [6] Lieb, E., Schultz, T. & Mattis, D. Two soluble models of an antiferromagnetic chain. *Annals of Physics* **16**, 407 – 466 (1961). URL <http://www.sciencedirect.com/science/article/pii/0003491661901154>.
- [7] Kim, E. H., Legeza, Ö. & Sólyom, J. Topological order, dimerization, and spinon deconfinement in frustrated spin ladders. *Phys. Rev. B* **77**, 205121 (2008). URL <http://link.aps.org/doi/10.1103/PhysRevB.77.205121>.
- [8] Hagymási, I. & Legeza, Ö. Characterization of a correlated topological Kondo insulator in one dimension. *arXiv [cond-mat.str-el]* 1601.04606 (2016). URL <http://arxiv.org/abs/1601.04606>. <http://arxiv.org/pdf/1601.04606>.
- [9] Haldane, F. D. M. Nonlinear field theory of large-spin Heisenberg antiferromagnets: Semiclassically quantized solitons of the one-dimensional easy-axis Néel state. *Phys. Rev. Lett.* **50**, 1153–1156 (1983). URL <http://link.aps.org/doi/10.1103/PhysRevLett.50.1153>.
- [10] White, S. R. Density matrix formulation for quantum renormalization groups. *Phys. Rev. Lett.* **69**, 2863–2866 (1992). URL <http://link.aps.org/doi/10.1103/PhysRevLett.69.2863>.
- [11] White, S. R. Density-matrix algorithms for quantum renormalization groups. *Phys. Rev. B* **48**, 10345–10356 (1993). URL <http://link.aps.org/doi/10.1103/PhysRevB.48.10345>.

- [12] Nielsen, M. A. & Chuang, I. L. *Quantum Computation and Quantum Information* (Cambridge University Press, 2000), 1 edn.
- [13] Bengtsson, I. & Życzkowski, K. *Geometry of Quantum States: An Introduction to Quantum Entanglement* (Cambridge University Press, 2006).
- [14] Petz, D. *Quantum Information Theory and Quantum Statistics* (Springer, 2008).
- [15] Ohya, M. & Petz, D. *Quantum Entropy and Its Use* (Springer Verlag, 1993), 1 edn.
- [16] Neumann, J. v. Thermodynamik quantenmechanischer gesamtheiten. *Nachrichten von der Gesellschaft der Wissenschaften zu Göttingen, Mathematisch-Physikalische Klasse* **1927**, 273–291 (1927). URL <http://eudml.org/doc/59231>.
- [17] Umegaki, H. Conditional expectation in an operator algebra. IV. entropy and information. *Kodai Math. Semin. Rep.* **14**, 59–85 (1962). URL <http://dx.doi.org/10.2996/kmj/1138844604>.
- [18] Hiai, F. & Petz, D. The proper formula for relative entropy and its asymptotics in quantum probability. *Commun. Math. Phys.* **143**, 99–114 (1991). URL <http://dx.doi.org/10.1007/BF02100287>.
- [19] Werner, R. F. Quantum states with Einstein–Podolsky–Rosen correlations admitting a hidden-variable model. *Phys. Rev. A* **40**, 4277–4281 (1989).
- [20] Modi, K., Paterek, T., Son, W., Vedral, V. & Williamson, M. Unified view of quantum and classical correlations. *Phys. Rev. Lett.* **104**, 080501 (2010). URL <http://link.aps.org/doi/10.1103/PhysRevLett.104.080501>.
- [21] Bennett, C. H., Bernstein, H. J., Popescu, S. & Schumacher, B. Concentrating partial entanglement by local operations. *Phys. Rev. A* **53**, 2046–2052 (1996). URL <http://link.aps.org/doi/10.1103/PhysRevA.53.2046>.
- [22] Bennett, C. H., DiVincenzo, D. P., Smolin, J. A. & Wootters, W. K. Mixed-state entanglement and quantum error correction. *Phys. Rev. A* **54**, 3824–3851 (1996). URL <http://link.aps.org/doi/10.1103/PhysRevA.54.3824>.
- [23] Szalay, Sz. Multipartite entanglement measures. *Phys. Rev. A* **7**, 042329 (2015). URL <http://link.aps.org/doi/10.1103/PhysRevA.92.042329>.

- [24] Szalay, Sz., Barcza, G., Szilvási, T., Veis, L. & Örs Legeza. The correlation theory of the chemical bond. *Scientific Reports* **7**, 2237 (2017). URL <https://www.ncbi.nlm.nih.gov/pmc/articles/PMC5440380/>.
- [25] Davey, B. A. & Priestley, H. A. *Introduction to Lattices and Order* (Cambridge University Press, 2002), second edn.
- [26] Stanley, R. P. *Enumerative Combinatorics, Volume 1* (Cambridge University Press, 2012), second edn.
- [27] Dür, W., Cirac, J. I. & Tarrach, R. Separability and distillability of multiparticle quantum systems. *Phys. Rev. Lett.* **83**, 3562–3565 (1999). URL <http://link.aps.org/doi/10.1103/PhysRevLett.83.3562>.
- [28] Dür, W. & Cirac, J. I. Classification of multiqubit mixed states: Separability and distillability properties. *Phys. Rev. A* **61**, 042314 (2000). URL <http://link.aps.org/doi/10.1103/PhysRevA.61.042314>.
- [29] Acín, A. *et al.* Generalized schmidt decomposition and classification of three-quantum-bit states. *Phys. Rev. Lett.* **85**, 1560–1563 (2000). URL <http://link.aps.org/doi/10.1103/PhysRevLett.85.1560>.
- [30] Seevinck, M. & Uffink, J. Partial separability and entanglement criteria for multiqubit quantum states. *Phys. Rev. A* **78**, 032101 (2008). URL <http://link.aps.org/doi/10.1103/PhysRevA.78.032101>.
- [31] Szalay, Sz. & Kökényesi, Z. Partial separability revisited: Necessary and sufficient criteria. *Phys. Rev. A* **86**, 032341 (2012). URL <http://link.aps.org/doi/10.1103/PhysRevA.86.032341>.
- [32] Szalay, Sz. Quantum entanglement in finite-dimensional Hilbert spaces. *arXiv [quant-ph]* 1302.4654 (2013). URL <http://arxiv.org/abs/1302.4654>. <http://arxiv.org/pdf/1302.4654>.
- [33] Östlund, S. & Rommer, S. Thermodynamic limit of density matrix renormalization. *Phys. Rev. Lett.* **75**, 3537–3540 (1995). URL <http://link.aps.org/doi/10.1103/PhysRevLett.75.3537>.
- [34] Dukelsky, J., Martín-Delgado, M. A., Nishino, T. & Sierra, G. Equivalence of the variational matrix product method and the density matrix renormalization group applied to spin chains. *EPL (Europhysics Letters)* **43**, 457 (1998). URL <http://stacks.iop.org/0295-5075/43/i=4/a=457>.

- [35] Schollwöck, U. The density-matrix renormalization group in the age of matrix product states. *Annals of Physics* **326**, 96 – 192 (2011). URL <http://www.sciencedirect.com/science/article/pii/S0003491610001752>. January 2011 Special Issue.
- [36] Affleck, I., Kennedy, T., Lieb, E. H. & Tasaki, H. Rigorous results on valence-bond ground states in antiferromagnets. *Phys. Rev. Lett.* **59**, 799–802 (1987). URL <http://link.aps.org/doi/10.1103/PhysRevLett.59.799>.
- [37] den Nijs, M. & Rommelse, K. Preroughening transitions in crystal surfaces and valence-bond phases in quantum spin chains. *Phys. Rev. B* **40**, 4709–4734 (1989). URL <http://link.aps.org/doi/10.1103/PhysRevB.40.4709>.
- [38] Wolf, M. M., Verstraete, F., Hastings, M. B. & Cirac, J. I. Area laws in quantum systems: Mutual information and correlations. *Phys. Rev. Lett.* **100**, 070502 (2008). URL <https://link.aps.org/doi/10.1103/PhysRevLett.100.070502>.
- [39] Barcza, G., Noack, R. M., Sólyom, J. & Legeza, Ö. Entanglement patterns and generalized correlation functions in quantum many-body systems. *Phys. Rev. B* **92**, 125140 (2015). URL <http://link.aps.org/doi/10.1103/PhysRevB.92.125140>.
- [40] Calabrese, P. & Cardy, J. Entanglement entropy and quantum field theory. *Journal of Statistical Mechanics: Theory and Experiment* **2004**, P06002 (2004). URL <http://stacks.iop.org/1742-5468/2004/i=06/a=P06002>.
- [41] FÁTH, G., Legeza, Ö., Lajkó, P. & Iglói, F. Logarithmic delocalization of end spins in the $s = \frac{3}{2}$ antiferromagnetic Heisenberg chain. *Phys. Rev. B* **73**, 214447 (2006). URL <http://link.aps.org/doi/10.1103/PhysRevB.73.214447>.
- [42] FÁTH, G. & Sólyom, J. Period tripling in the bilinear-biquadratic antiferromagnetic $s=1$ chain. *Phys. Rev. B* **44**, 11836–11844 (1991). URL <https://link.aps.org/doi/10.1103/PhysRevB.44.11836>.
- [43] Xian, Y. Exact results of dimerization order parameter in $su(n)$ antiferromagnetic chains. *Physics Letters A* **183**, 437 – 440 (1993). URL <http://www.sciencedirect.com/science/article/pii/037596019390602V>.
- [44] FÁTH, G. & Sólyom, J. Search for the nondimerized quantum nematic phase in the spin-1 chain. *Phys. Rev. B* **51**, 3620–3625 (1995). URL <http://link.aps.org/doi/10.1103/PhysRevB.51.3620>.

- [45] Legeza, Ö., Fáth, G. & Sólyom, J. Phase diagram of magnetic ladders constructed from a composite-spin model. *Phys. Rev. B* **55**, 291–298 (1997). URL <http://link.aps.org/doi/10.1103/PhysRevB.55.291>.
- [46] Kawashima, N. Quantum Monte Carlo methods. *Progress of Theoretical Physics Supplement* **145**, 138–149 (2002). URL <http://ptps.oxfordjournals.org/content/145/138.abstract>. <http://ptps.oxfordjournals.org/content/145/138.full.pdf+html>.
- [47] Chubukov, A. V. Fluctuations in spin nematics. *Journal of Physics: Condensed Matter* **2**, 1593 (1990). URL <http://stacks.iop.org/0953-8984/2/i=6/a=018>.
- [48] Legeza, Ö. Kvantuminformáció-elmélet alkalmazása erősen korrelált rendszerek vizsgálatára és az ERA koncepció (2012). DSc thesis.
- [49] Legeza, Ö. QC-DMRG-Budapest, a program for quantum lattice and chemical DMRG calculations. (2012).
- [50] MATLAB. *version 8.6.0 (R2015b)* (The MathWorks Inc., Natick, Massachusetts, 2015).

NYILATKOZAT

Név: Máté Mihály

ELTE Természettudományi Kar, szak: fizikus MSc

NEPTUN azonosító: N3Y91O

Diplomamunka címe:

Simulation of strongly correlated systems with tensor network state methods

A **diplomamunka** szerzőjeként fegyelmi felelősségem tudatában kijelentem, hogy a dolgozatom önálló munkám eredménye, saját szellemi termékem, abban a hivatkozások és idézések standard szabályait következetesen alkalmaztam, mások által írt részeket a megfelelő idézés nélkül nem használtam fel.

Budapest, 2017. május 31.

a hallgató aláírása